ULTRA-POROUS INTERCONNECTED HYDROGEL STRUCTURES FOR TISSUE ENGINEERING APPLICATIONS

A Thesis Submitted to
the Graduate School of Engineering and Sciences of
İzmir Institute of Technology
in Partial Fulfillment of the Requirements for the Degree of

MASTER OF SCIENCE

in Chemistry

by
Büşra YILDIZ

December 2018
İZMİR

We approve the thesis of **Büşra YILDIZ**

Examining Committee Members:

Assoc. Prof. Dr. Ümit Hakan YILDIZ
Department of Chemistry, İzmir Institute of Technology

Prof. Dr. Mustafa M. DEMİR
Department of Materials Science and Engineering, İzmir Institute of Technology

Assist. Prof. Dr. Nesrin Horzum POLAT
Department of Engineering Sciences, İzmir Katip Çelebi University

14 December 2018

Assoc. Prof. Dr. Ümit Hakan YILDIZ
Supervisor,
Department of Chemistry
İzmir Institute of Technology

Assist. Prof. Dr. Ahu ARSLAN YILDIZ
Co-Supervisor,
Department of Bioengineering
İzmir Institute of Technology

Prof. Dr. Ahmet Emin EROĞLU
Head of the Department of Chemistry

Prof. Dr. Aysun SOFUOĞLU
Dean of the Graduate School of
Engineering and Sciences

ACKNOWLEDGMENTS

First of all, I would like to thank my supervisor Assoc. Prof. Dr. Ümit Hakan Yıldız and co-supervisor Assist. Prof. Dr. Ahu Arslan Yıldız for their guidance, suggestions, patience, encouragement and support throughout my thesis study.

I would like to thank Assoc. Prof. Dr. Engin Karabudak and their laboratory members to support me for using UV curing machine in my experiments.

I also thank to specialists at IZTECH Center of Material Research for the SEM anaylsis.

I would like to thank Rabia Önbaş for her help with cell culture analysis, Sezer Özenler, Rümeysa Bilginer, Mustafa Umut Mutlu, Müge Yücel and all members of the BioSens&BioApps and Biomimetics groups for their friendship and aids during my studies.

Besides, I am very grateful to my lovely friends Seray Ece Keskin, Özlem Ece, Özge Tüncel and İlayda Melek Yırtıcı for their encouragements and supports.

Finally, I would like to offer my special thanks to my family especially to my mother. I am very grateful to my beloved husband Talha Enes Köksal for his all aids in my thesis studies and career.

I am very pleasant to dedicate my thesis to my beloved husband Talha Enes Köksal and our family.

ABSTRACT

ULTRA-POROUS INTERCONNECTED HYDROGEL STRUCTURES FOR TISSUE ENGINEERING APPLICATIONS

Tissue engineering aims to repair and regenerate tissue and organs with functional defects. The most significant developments in tissue engineering emerging as modification of the scaffold used to mimic native extracellular matrix (ECM) and support cell proliferation and differentiation. Hydrogel-based biomaterials are one of the most utilized materials as scaffold providing excellent chemical, physical/biophysical properties, high biocompatibility and functionality necessary for the applications in tissue engineering. In this study, Gelatin methacryloyl hydrogel (GelMA) and Gelatin-urethane hydrogels (GelatinK) are successfully synthesized as scaffold material for tissue engineering applications. Gelatin is modified with methacrylic anhydride for GelMA polymer and with 2-isocyanatoethly methacrylate for GelatinK polymer. The hydrogels of these two novel polymer are produced with photopolymerization reactions in aqueous media using Irgacure 2959 as redox initiator. Hydrogels are freeze-dried to remove solvent in the gel matrix and then they immersed in distilled water to reach equilibrium swelling ratio. The swelling capacity of GelMA hydrogels ranges between 1200 and 300% whereas GelatinK hydrogels has swelling capacity in between 1900-380%. Also, morphology of the hydrogels were investigated with Scanning Electron Microscopy (SEM). GelMA hydrogels has pore sizes between 142-14 μm while GelatinK hydrogels has between 160-56 μm pore sizes. The cell viability assay were also conducted using GelMA and GelatinK hydrogels. The results showed that both hydrogels provide high viability as compared to 2D control assay.

ÖZET

DOKU MÜHENDİSLİĞİ UYGULAMALARI İÇİN BİRBİRİNE BAĞLI AŞIRI GÖZENEKLİ HİDROJEL YAPILAR

Doku mühendisliği fonksiyonel bozukluğu olan doku ve organları tedavi etmeyi ve yenilemeyi amaçlar. Doku mühendisliğindeki en önemli gelişmeler hücre dışı matrisi taklit eden ve hücre çoğalmasını ve farklılaşmasını destekleyen doku iskelesinin değiştirilmesi olarak ortaya çıkmaktadır.. Doku mühendisliği uygulamaları için gerekli olan mükemmel kimyasal, fiziksel/biyofiziksel özellikleri, yüksek biyouyumluluğu ve fonksiyonelliği sağlayan hidrojel temelli biyomalzemeler iskele olarak en çok kullanılan malzemelerden biridir. Bu çalışmada, Jelatin metakriloyil hidrojeli (GelMA) ve Jelatin-urethan hidrojelleri (GelatinK) doku mühendisliği için iskele malzemesi olarak başarılı bir şekilde sentezlenmiştir. Jelatin, GelMA polimeri için metakrilik anhidrit ile ve GelatinK polimeri için 2-izosiyanatoetil metakrilat ile değiştirilmiştir. Bu iki yeni polimerin hidrojelleri fotopolimerleşme yöntemiyle Irgacure redoks başlatıcısı kullanılarak su ortamında üretilmiştir. Jel matriksindeki çözücüyü uzaklaştırmak için hidrojeller dondurularak kurutulmuş ve şişme dengesine ulaşmaları için distile su içerisine atılmıştır. GelMA hidrojellerinin şişme kapasitesi 1200 ve 300% arasında iken GelatinK hidrojelleri 1900-380% arasında şişme kapasitesine sahiptir. Ayrıca, bu hidrojellerin morfolojisi taramalı electron mikroskopisi (SEM) ile incelenmiştir. GelMA hidrojeleri 142-14 μm arasında gözenek boyutuna sahipken GelatinK hidrojelleri 160-56 μm pore boyutuna sahiptir. Hücre canlılığı denemeleri de GelMA ve GelatinK hidrojelleri kullanılarak yönetilmiştir. Sonuçlar her iki hidrojelin de 2 boyutlu kontrol denemelerine kıyasla yüksek hücre canlılığına sahip olduğunu göstermiştir.

TABLE OF CONTENTS

LIST OF FIGURES

LIST OF TABLES

CHAPTER 1

INTRODUCTION

1.1. Extent of Thesis

GelMA and Gelatin-Urethane hydrogels were synthesized to mimic the native extracellular matrix with its natural physical and biochemical properties. Hydrogels were produced with photopolymerization reactions in aqua conditions. Here we synthesized a novel polymer modifying gelatin with 2-isocyanatoethyl methacrylate and then hydrogels of this polymer were produced under UV curing. The hydrogels were investigated to understand the swelling capacity and porous morphology. The hydrogels were used for further 3D cell culture experiments.

1.2. Hydrogels for Tissue Engineering

The future aspect in design and synthesis of bioinspired materials are not simply mimicking their natural counterparts but providing phenomenal properties and advancements that even recover deficiency of nature made matter. The gels are one of the most studied soft matter utilized in varying biotechnological application such as tissue engineering, therapeutic agent carrier and delivery, diagnostic, bioimaging and biosensing. The synthetic gels have been dramatically evolved to provide broad functionality, stability and responsiveness as well as low toxicity that synchronizes abilities of polymer science, biology, pharmaceutical sciences and bioengineering. Therefore the use of hydrogels is getting a golden standard for tissue engineering applications since they provide excellent biocompatibility, mechanical strength as well as responsiveness.

1.2.1. Hydrogels

The term ‘’ gel’’ refers to a material in which a liquid phase and a solid phase are dispersed in each other and forms a three dimensional (3D) structure. The gels are

primarily classified as natural and synthetic gels that natural or biomimetic gels have natural origins. The gels mimic the extracellular matrix (ECM) are most frequently used in biomedical applications. The weak mechanical strength of these gels have directed the scientists to synthesize hybrid gels which is a combination of biomimetic and synthetic gels. Gels are classified in terms of different aspects such as their responsive behaviors, the nature of monomer, crosslinking and liquid phase. Figure 1.1 illustrates the classification of gels.

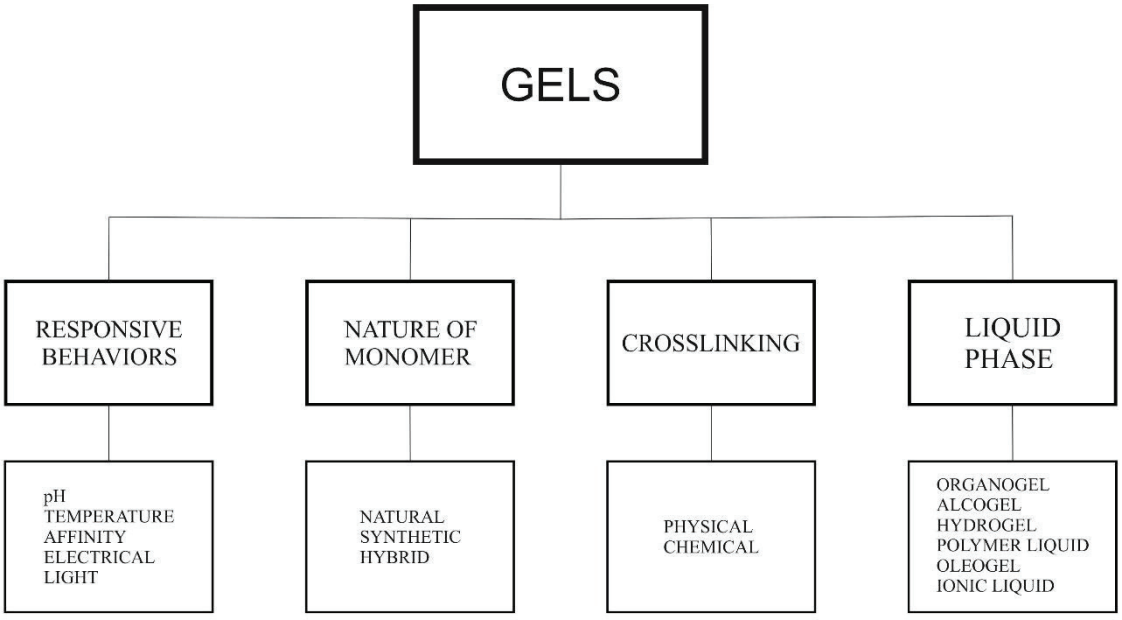

Figure 1.1 The classification of gels based on their responsive behaviors, nature, crosslinking type, liquid phase.

The gels are mainly categorized as pH [1-2], temperature [3-4], affinity [5-6], electrical field [7-8] and light responsive [9-10]. The hydrogels are able to sense the variations in these stimuli and capable of responding more than one stimuli giving dual or multi responsivity [11-14]. The natural, synthetic and hybrid hydrogels are classified based on the nature of building blocks. Natural hydrogels can be composed of chitosan [4, 15], alginate [16-18], collagen [19-20], gelatin [21-23], fibrinogen [24], dextran [25-26] and hyaluronic acid [27-28] to mimic the nature of tissues for different applications.

1.2.1.1. Swelling Ability of Hydrogels

The swelling of gels occurs by absorbing a large amounts of water while preserving their 3D structure called as volume-phase transition. The swelling is primarily governed by the diffusion of water molecules into the space between hydrogel networks (chain) depending on the interactions of polymer chain and water. Ionic nature and hydrophilicity of the chain are the main parameters affecting the polymer-water interaction. As represented in Figure 1.2, stimuli responsive gels swell or collapse in the presence of specific environmental effects. Solvent molecules diffused into the gel matrix depending on the morphology and backbone structure of gel. In collapsed state, solvent molecules released from matrix and gel becomes dry state.

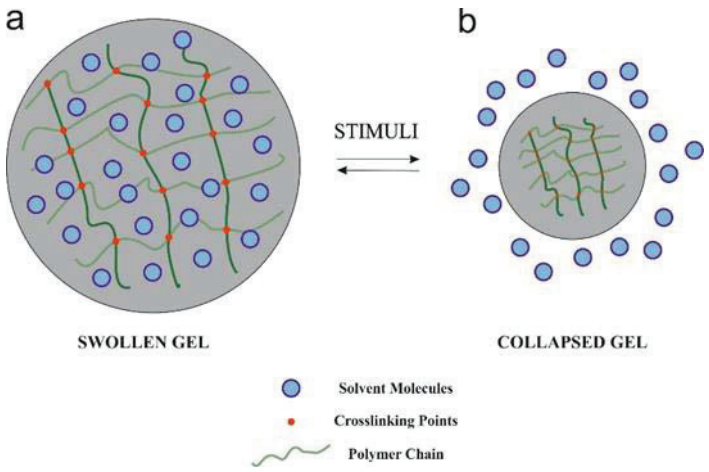

Figure 1.2 Swelling and shrinking of a gel in response to different stimuli. (a) Swollen gel contains solvent molecules diffused between polymeric chains; (b) Swollen gel shrink to collapsed state by releasing solvent molecules to surrounding when external stimuli is applied.

The swelling of anionic and cationic polymers following opposite pathways. As shown in Figure 1.3, in basic media, anionic poly (acrylic acid) (PAA) becomes deprotonated and swells whereas cationic poly (N, N 9-diethylaminoethyl methacrylate) are protonated and thus shrink by decreasing water content. Acidic conditions give rise to shrinking of PAA and swelling of poly (N, N 9-diethylaminoethyl methacrylate) hydrogels. This unique property of gels have been exploited for various pharmaceutical applications for instance, Liu et al. designed a sericin/dextran (SDH) injectable hydrogel crosslinked with hydrazone and loaded with Doxorubicin to prevent tumor growth. The

swelling experiments were carried out in PBS at varying pHs; 6.0, 7.4 and 11.0 at 37 °C. When DEX-Al content increased, the swelling degree of hydrogels fell. This decline may result of the lower pore size and porosity of gel in formulations with lower percent of sericin. In acidic conditions, pH 6.0 which is near to isoelectric point of sericin, swelling decreased compared to basic conditions [26].

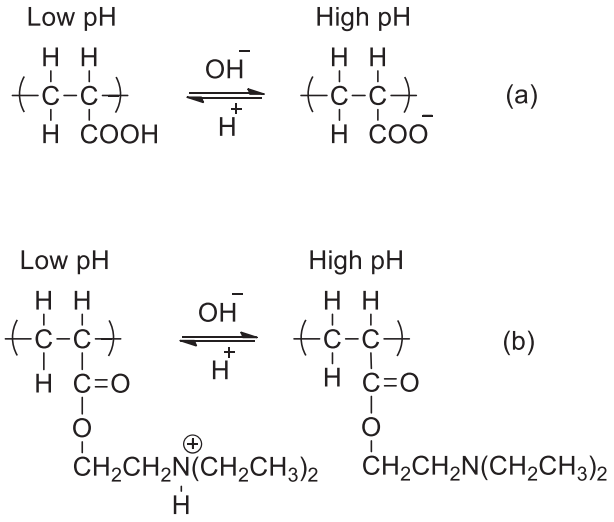

Figure 1.3 Ionization of a) Poly (acrylic acid) and b) poly (N, N'-diethylaminoethyl methacrylate) responding to pH of environment.

1.2.1.2. Responsive Behaviors of Hydrogels

The volume-phase transition is considered to be major mechanism governed by either "osmotic pressure and charge density alterations" or "affinity of the backbone to the solvent" providing stimuli responsive behavior of gels. The stimuli responsive gels are found to be that sensitive to changes in environmental effects such as temperature, pH, electrical field, affinity and light [29-33]. Some of these stimuli are within in living body such as pH, temperature, chemical species and biomolecules, thus these systems have potential to be implemented to body for varying applications. Figure 1.4 represents these stimuli responsivity of gels to different environmental effects.

pH Responsive gels sense the alterations in pH of the surrounding medium and thus swell or shrink in volume. pH responsivity is provided by the ionic groups on the backbone of gels. The polyelectrolytes with varying ionizable functional groups in the backbone lead to repulsion between polymer chains.

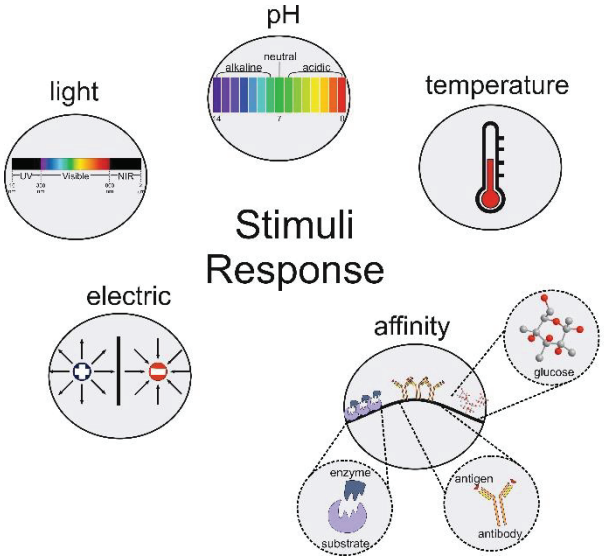

Figure 1.4 Stimuli responsivity of gels to the different effects; light, pH, temperature, electric and affinity (enzyme, glucose, antigen and antibody).

This repulsion forms a space for water to diffuse and swell. Conversely, the space can dwindle from initial state and water removes to shrink. The pH responsive gels were well exploited in various applications. For instance Manchun et al. have developed pH-responsive dextrin nanogels (DNGs) to deliver doxorubicin (DOX) into specific tumor site in treatment of colorectal cancer [34]. Alginate/κ-carrageenan composite hydrogel beads were synthesized as a pH-responsive insulin aspart carrier agent. The gel was obtained by gelation of alginate and κ-carrageenan in the presence of insulin and Ca^{2+} as gelling agent. The hydrogel beads with 1% w/v of κ-carrageenan showed swelling degree 8%, - 43% and around 120% in water, SGF (pH 1.2) and SIF (pH 7.4) respectively after 6h incubation. - 43% swelling means that gel beads collapsed due to hydrogen bonding [35]. Also, a supramolecular hydrogel based on cellulose and gelatin was produced. pH responsiveness of the hydrogel was observed in pH from 2.0 to 11.0. When pH increase from 2.0 to 5.0, water uptake ratio decreased, pH range between 5.0-8.0 caused swelling degree to rise due to high electrostatic repulsive forces between gelatin and cellulose. After pH 8.0 swelling declined because amino group of gelatin was deprotonated and water uptake capacity lowered. These results showed pH responsive behavior of the hydrogel system [36].

Temperature-sensitive hydrogels exhibit a change in volume based on the temperature of the environment. These gels usually contains hydrophobic or both hydrophilic and hydrophobic groups on polymer backbone. Temperature responsive

hydrogels are positive or negative responsive based on upper critical solution temperature (UCST) or a lower critical solution temperature (LCST), respectively. On the other hand, gels with physically crosslinking can response to temperature changes by sol-gel phase transitions instead of swelling and deswelling mechanisms. The transition from sol to gel occur above at a specific temperature (LCST) due to the solidification of polymers being hydrophobic at this condition. The sense action of the positive responsive hydrogels depends on the UCST. Expand in volume of hydrogel occurs if the temperature is higher than UCST. These gels becomes unswollen by releasing the temperature below. Gels with low critical solution temperature (LCST) can absorb water at the temperature below the LCST and release water when temperature rise from the LCST [37].

Poly (N-isopropylacrylamide) (PNIPAAm) is a well-known thermoresponsive hydrogel with lower critical solution temperature (LCST) or transition temperature at ~31-32 ºC [38-39]. Also, Liu et al. synthesized the hydrogels of N-isopropylacrylamide (NIPA), sodium acrylate (SA) and sodium methacrylate (SMA) in aqueous solution with free radical polymerization technique. The swelling and deswelling measurements at different temperatures (beginning from room temperature to maximum 60 ºC and reverse for deswelling experiment) demonstrated that swelling and deswelling of the hydrogels were reversible meaning these gels are thermoresponsive [40].

An affinity responsive gels respond to large biological macromolecules as well as to small chemical constructs. Smart gels responding the target biomolecules show volume changes making the gel system appropriate for varying biomedical applications. To target the biomolecule, gels are combining with the biomolecular recognition sites during the synthesis. These gels were developed to be responsive to glucose, proteins, antigens and other type of biomolecules. There are different approaches to make hydrogels as glucose responsive material such as entrapping glucose-oxidase (Gox), phenylboronic acid and its derivatives, and lectins. Entrapping glucose oxidase into the gel system is one of the most used methodology. In such a system, glucose is oxidized to gluconic acid, catalyzed by Gox and the pH inside the microenvironment decreases with the increase in the glucose concentration. This causes an increase in the volume of the pH sensitive hydrogel, which results in the release of entrapped insulin [41].

Glucose sensitive hydrogels are prepared based on the complex formed between phenylboronic acid and polyols which have a stronger affinity for phenylboronic acid. A triple (pH, temperature and glucose) responsive P (DMAEMA-co-AAPBA) hydrogels are produced by copolymerization of (2-dimethylamino) ethyl methacrylate (DMAEMA)

and 3-acrylamidephenylboronic acid (AAPBA) by Wang and co-workers. Depending on the glucose concentrations at 37 °C, the hydrogels become swollen with different water uptake ratios. This result proof the suitability of P(DMAEMA-co-AAPBA) hydrogels for glucose sensitive carrier systems [12]. Xiong et al. have developed bacteria-responsive multifunctional nanogels in order to deliver antibiotic to bacterial infection sites. The antibiotic release is stimulated with bacterial enzymes by degrading polyphosphoester core of the nanoparticle and transported to bacterial infection sites. Thus the antibiotic is released and the bacterial growth inhibition is enhanced. Drug activation in situ and macrophages targeting properties make bacteria-responsive nanogels significant for delivery of antibiotics in the treatment of bacterial infectious diseases [42]. Hydrogels sensing the antigen-antibody interactions by swelling and deswelling mechanisms have been attracted by many biomedical applications like biosensing and immunotherapies. These systems are designed by physically interactions of antibody or antigen with polymeric backbone, chemical modifications of the backbone with these species, and reversible crosslinking of hydrogel with antigen-antibody interactions [30].

Gels with electro-sensitive functional groups, demonstrate volume changes in response to electrical field. There are many examples of electro-responsive gel systems used in different fields like polyvinyl alcohol/poly (sodium maleate-co-sodium acrylate), chitosan/carboxymethylcellulose hydrogel, chitosan-g-poly (acrylic acid) hydrogel elastomers, polyacrylic acid/fibrin hydrogel [8, 43-45]. Gao et al. synthesized electro-responsive starch hydrogels by crosslinking with glutaraldehyde. Response of the gel showed rising with increasing strength of electrical field. Efficient response was observed around 1.2 kV/mm. It is concluded that electrical field applied and starch concentration in hydrogel formulation affect the electro-sensitivity of material [46].

Hydrogels that carry light-sensitive functional groups on the structure are able to swell or deswell based on the light, UV or visible, subjected to the material [47]. Kang et al. developed near-infrared light-responsive nanogel system based on Au-Ag nanorods (Au-Ag NRs) coated with DNA cross-linked polymeric for targeted delivery of drugs. DNA cross-linked polymeric shells are developed to encapsulate anticancer drugs into the gel scaffold while Au-Ag NRs are easily functionalized with targeting moieties for identifying cancer cells. Thus, the encapsulated drug is released with high controllability after dissolving of the coated gel shells. The light-responsive gel system were used remote controlled targeted drug by NIR light [48]. Poly(N-isopropylacrylamide) microgels, poly(N-isopropylacrylamide)-b-poly(4-acryloylmorpholine)-b-poly(2-((((2-

nitrobenzyl)oxy)carbonyl) amino)ethyl methacrylate) (PNIPAM-b-PNAM-b-PNBOC) hydrogels, semi IPN hydrogels based on β -cyclodextrin-grafted alginate (β-CD-Alg) and diazobenzene-modified poly(ethylene glycol) (Az2-PEG) gel systems are another examples of photoresponsive gels [9, 11, 49]. Hang et al. created degradable NIR and UV-responsive nanogels from hyaluronic acid-g-7-N, N-diethylamino-4-hydroxymethylcoumarin (HA-CM) due to their tendency to target CD44+ tumor cells and to be able to control the transmission of doxorubicin (DOX) into these cells. The nano-sized and light-responsive particles, (HA-CM) were easily load DOX and drug releases into tumor cells is activated by NIR and UV irradiation. The light responsive nanogels provide significant improvements in cancer chemotherapy [10].

1.2.1.3. Mechanical Behaviors of Hydrogels

The mechanical property of gels is one of the most vital points when these gels are applied for a specific goal. Elastic recovery and the time-dependent recovery of hydrogels are crucial and based on viscous behaviors [50]. The rubber can be given as an example for a polymer backbone. Rubbery behavior of gels indicates high ability to deformation and complete recovery. They are subjected to large deformations and can back to original states without fractures. The deformation due to an external force and the elasticity of polymer are highly dependent to chemical composition and structure of the polymer network. Elastic modulus of the material gives substantial information about the polymer network and stiffness. The elastic behavior of polymer is affected by several factors like network structure, monomer composition, crosslinking degree, swelling, ionic groups on backbone and entanglement [51-54]. Modified reagents at the different ratio in the gel compounds lead to dramatic changes of mechanical properties of resulting gels.

Coutinho et al. modified Gellan Gum (GG) with methacrylate groups in order to increase mechanical properties at physiological conditions used in tissue engineering. Thus GG hydrogels can be crosslinked by both physical and chemical mechanisms when methacrylate groups were integrated into the GG chain. Young's modulus values of hydrogels with different crosslinking ratios were observed to between 0.15 and 148 kPa [55]. Hachet et al. modified hyaluronic acid which is a natural polysaccharide abundant in biological tissues with methacrylate in order to allow real time monitoring of gelation during photopolymerization. The effect on the gel properties was adjusted by the complete conversion of the methacrylate groups and conversion of all methacrylate

groups was taken advantage of biomimetic hydrogel substrates for 2-dimensional cell culture [56]. You et al. synthesized Quaternized chitosan (QCh) and polyelectrolyte complex (PEC) hydrogels. The relationship between hydrogel structure and mechanical properties was examined because charge density and the concentration of QCH gave the property of tough with self-recovery properties. The author claim that the tensile fracture nominal stress (σb) and work of extension at fracture (Wb) value 16.1 MPa and 15.6 MJ/m^3, respectively. The results indicate that considerable potential arise for application in load-bearing artificial soft tissues [57].

De France et al. create in situ gelling nanocomposite hydrogels based on hydrazone cross-linked poly(oligo-ethylene glycol methacrylate) (POEGMA) and rigid rod-like cellulose nanocrystals (CNCs) in order to improve injectable hydrogel's mechanical properties. Within the addition of CNCs the storage moduli are increased (up to 35-fold increases in storage modulus) and it is suitable for high strength biodegradable tissue engineering scaffolds [58]. Also, chain entanglement is using design to create highly tunable physical and mechanical properties such as protein hydrogels based on coiled-coil interactions. Tang et al. creates coupling the cysteine residues near the N- and C-termini in order to obtain chain entanglement that has reversible properties thanks to disulfide bonds. The results indicate that hydrogels which are with a toughness of 65 000 $J\ m^{-3}$ and extensibility to approximately 3000% engineering strain are mimic tendon and cartilage in sense of high toughness [59].

1.3. Tissue Engineering

Tissue engineering hold the promises to repair and regenerate damaged tissues or organs by improving functions. It is an interdisciplinary area uses the principles of many different areas like engineering and life sciences to construct biological substituents [60]. With the progress in regenerative medicine and tissue engineering artificial tissue and organ models can be designed with novel fabrication techniques [61-62]. Tissue engineering uses scaffolds to mimic native extracellular matrix (ECM) for directing cells to regenerate function of tissue and organs. Cells and other functional biomolecules are also integrated into tissue models [63].

The major fragment in tissue engineering is the usage of proper scaffold to organ or tissue need to be repaired or replaced. Soft materials hold the potential to fabricate constructs that mimic the native microenvironment and complexity of tissues and organs

better than any other counterpart. Advances in soft biomaterials have supported the rapid development of applications in biotechnology and biomedicine. Hydrogel-based soft-materials have attracted great interest due to their excellent chemical, physical/biophysical properties, and functionalities suitable for constructing 3D biomaterials.

Hydrogel-based biomaterials are one of the most utilized materials providing high biocompatibility and functionality necessary for the applications in biotechnology and biomedicine in different aspects. Hydrogels with optimized chemical and physical properties, and structures have been especially used for biofabrication of desired 3D constructs [62, 64]. Responsiveness towards different stimuli, low toxicity and mechanical properties of hydrogels are also attractive features for biological applications [50].

Over the past several decades, utilization of hydrogels for in vitro tissue model fabrication attracted great attention since biocompatibility, high efficiency to encapsulate bioactive molecules and cells, delivery of therapeutic agents and effective mass transfer through the constructed tissue are all important features provided by hydrogels [65-67]. Natural and synthetic hydrogels composed of collagen, alginate, gelatin, chitosan, poly(vinyl alcohol) (PVA), poly(ethylene glycol) (PEG), and poly(lactic-co-glycolic acid) (PLGA) have been widely used to investigate cell-cell and cell-extracellular matrix (ECM) interactions. Natural hydrogels make the material more biocompatible while synthetic hydrogels give mechanical strength to construct as required to obtain native-like tissue models [47, 68-73].

Biofabrication process of hydrogel-based materials can be classified in two subgroups; as conventional and advanced manufacturing techniques [74]. In conventional techniques, 3D scaffolds can be designed without a complex and costly instrument. These techniques are freeze-drying [75-76], gas foaming [77-78], solvent casting [79-80] and cryogelation [81-82]. Major limitations of the use of these techniques can be explained as; scaffolds fabricated with traditional methods can be lack of interconnected and uniform pores, and using toxic organic solvents are one of the possible disadvantages for bio-related applications. Also microarchitecture and properties of the scaffold may not be tunable to desired tissues and other biological constructs [83-84]. To overcome the disadvantages that arise from the limitations of conventional techniques, advanced manufacturing techniques were utilized most of the time. Advanced manufacturing techniques are able to incorporate biological parts like cell, genes, and nucleotides into a biomaterial to design tissue or organ models at high resolutions. Advanced techniques that are utilized for

hydrogel processing, classified as; electrospinning [85-86], micromolding [87-88], microfluidic systems [89-90] and bioprinting [91-93]. The control over the process and biomaterial determines the morphology, microarchitecture and eventually efficiency of the material in desired bioapplication like tissue engineering and regeneration, 3D cell culture, biopreservation and gene therapy.

1.4. Applications of Hydrogels

The specific and excellent responsivity of gels to the different stimuli, swelling properties and porous structure make the gels very attractive in many fields such as biomedicine, pharmaceutical industry, biotechnology, environmental applications, agriculture and biosensors [37]. Hydrogels are mostly used in therapeutic agent delivery systems [94-99], diagnostic and imaging systems [100-103], biosensor applications [104-107] and tissue engineering techniques as scaffold for tissue and organ models .

Over the years therapeutic agent delivery with gel-based cargoes are becoming more effective for treatment of diseases and especially outpatient treatments. These therapeutic agents can be drugs [108-109], proteins [110] and genetic materials [111]. In these therapies, the biocompatibility, biodegradability and responsive and swelling behaviors of the gels are crucial to obtain a convenient cure. The material properties of the carrier agent and the interactions between the gel and the therapeutic agent have to be well understood before applying to drug formulations. Drug carrier hydrogels obtained by encapsulation or dissolution of therapeutic agent in the hydrogel just like hydrogels loaded with protein and bounding by electrostatic interactions between the hydrogel and the cargoes [112-114]. For example, hydrophilic gemcitabine (GCT) and hydrophobic doxorubicin (DOX) drugs were loaded into poly (N-isopropylacrylamide)-b-poly (4-acryloylmorpholine)-b-poly (2-((((2-nitrobenzyl) oxy) carbonyl) amino) ethyl methacrylate) (PNIPAM-b-PNAM-b-PNBOC) copolymer hydrogels which are sensitive to UV irradiation and temperature. When the temperature is below the lower critical solution temperature (LCST), the hydrogels self-assembled to a micelle structure in which photo-responsive PNBOC part in the core, hydrophilic PNAM moiety in inner, and thermos-sensitive coronas with PNIPAM chains. Delivery of GCT and DOX drugs were also achieved by this responsive manner [11].

Simplicity of formation, biocompatibility, and high stability of hybrid micro nanogels make them useful for chemical and biochemical sensing and disease diagnoses.

The monitoring of the biochemistry and biophysics of live cells over time and space are facilitated by hybrid micro nanogels' intracellular probing ability, therefore they make contribution to the explanation of intricate biological processes and the progress of novel diagnoses [41]. Hui Xu et al. developed an assay for multiplex detection of Down's syndrome which is based on inverse opal structure hydrogel barcodes with poly (ethylene glycol) diacrylate (PEG-DA), poly (ethylene glycol) (PEG) and acrylic acid (AA) hybrid components. The stabilities of the inverse opal structure is provided by the polymerized (PEG-DA) hydrogel, the interconnected pores of the inverse opal structure induced by (PEG) supply channels for biomolecules to diffuse into the voids of whole barcodes and, the probe immobilization is provided by (AA) [115]. Chitosan− carbon dot (CD) nontoxic hybrid nanogels (CCHN) can be incorporated by pH-sensitive chitosan and fluorescent CDs into a single nanostructure for near-infrared imaging (NIR) and NIR/pH dual-responsive drug release to develop therapeutic efficacy [116].

Physical properties of hydrogel make it very responsive to certain stimuli such as pH, temperature, light [117]. That stimuli responsive characteristic of hydrogel is proper for biosensing mechanism in the field of biotechnology, drug delivery and tissue engineering [118-120]. Biological modified hydrogels are good candidates for biosensing application due to its thermodynamically favorable interactions [121]. Srinivas et al. synthesize microgel particles for protein detection. They prepare a monomer solution by mixing poly (ethylene glycol) diacrylate, poly (ethylene glycol), Darocur 1173 and 3X Tris-EDTA buffer with different ratios. The microgel particles are then functionalized with specifically modified DNA aptamers. They claim that the assay is highly sensitive to human α-thrombin, which is important for diagnosis of cardiovascular disorders, with a limit of detection of 4 pM [122].

Gelatin is a protein based polymer obtained by hydrolytically degradation of collagen which is the main fibrous protein constituent in bones, cartilages and skins and the most abundant protein in ECM [123-124]. Thanks to high water solubility, cell adhesive ability, biocompatibility, low immunogenicity and low cost, gelatin is widely used in hydrogel formulations for tissue engineering applications [125]. Figure 1.5 demonstrates the protein structure of gelatin and amino acid groups on gelatin backbone. The RGD sequences promotes cell attachment and biocompatibility of gelatin based hydrogels. In general, gelatin is modified by other functional groups or combined with different polymers to increase durability and mechanical strength of gelatin-based hydrogels. Gelatin methacryloyl (GelMA) hydrogels have gained high attentions in tissue

engineering applications. Using redox initiator, GelMA gets photopolymerization reactions leading to chemically crosslinked GelMA hydrogels. Generally, gelation occurs with UV curing in the presence of Irgacure 2959 as common redox initiating agent [126]. Loessner and co-workers fabricated gelatin methacryloyl (GelMA) and hyaluronic acid methacrylate (HAMA) hydrogels via casting pre-polymer solution into Teflon mold. UV cure at 365 nm was applied to crosslink hydrogels. The produced hydrogels were examined as 3D scaffolds for ovarian, breast, and prostate cancers, as well for vascular network formation, and cartilage tissue engineering [127].

GelMA and carboxybetaine methacrylate (CBMA) based hydrogels were synthesized to obtain stiffer hydrogels for controlled drug release. Incorporation of CBMA increased mechanical strength, decrease degradation rate as compared to GelMA hydrogel. SEM images showed open pore microstructure and interconnected pores of the hydrogels with 100-150 μm pore diameters. Swelling ratio was observed between 895 and 1058%. Mechanical strength of the hydrogel was determined with stress-strain curves from compression tests. The average compressive moduli of hydrogels were between almost 16 and 36 kPa. Incorporation of CBMA in 5% ratio increased mechanical strength of hydrogel from 16 to 36kPa. Also, the hydrogels showed high cell viability proofing biocompatibility of the hydrogel for drug release and tissue engineering [128].

Saraiva et al. produced chitosan methacrylamide (ChMA) and GelMA hydrogels with photopolymerization using Irgacue 2959 as photoinitiator. SEM images showed interconnected but nonhomogeneous pores on hydrogel surface. Average pore size for ChMA:GelMA (2:1) and 1:1 was 30 μm and 3 μm respectively. Swelling ratio of the hydrogels after one hour was 1823% and 997% for ChMA: GelMA with (2:1) and 1:1 ratio. Swelling degree increased with increasing ChMA content due to hydrophilic nature of ChMA and protonation of amine groups on chitosan backbone [129]. Additionally, hydroxyapatite (HAP) and whitlockite (WH) minerals were incorporated to GelMA hydrogel, further fabricated composite hydrogels were used to encapsulate MSCs for bone tissue formation. The scaffold with the ratio of 3:1 (HAP: WH) was found to be most suitable one due to maximized osteogenic activity of MSCs. The ratio of the minerals is vital for mimicking the natural microenvironment of bone tissue with similar mechanical strength and osteogenic capacity [130].

Gelatin based hydrogels are commonly used to create tissue and organ models using advanced manufacturing techniques. GelMA[131-135], Fibrin/Gelatin[90] , Matrigel and Gelatin microparticles[136], chitin nanofibers/GelMA[137], alginate/GelMA[138],

GelMA/DexMA(Dextran methacryloyl)[139] and poly(glycerol sebacate) (PGS)–poly("-caprolactone) (PCL) microfiber reinforced methacrylated hyaluronic acid/GelMA hydrogels [140] are examples from the literature.

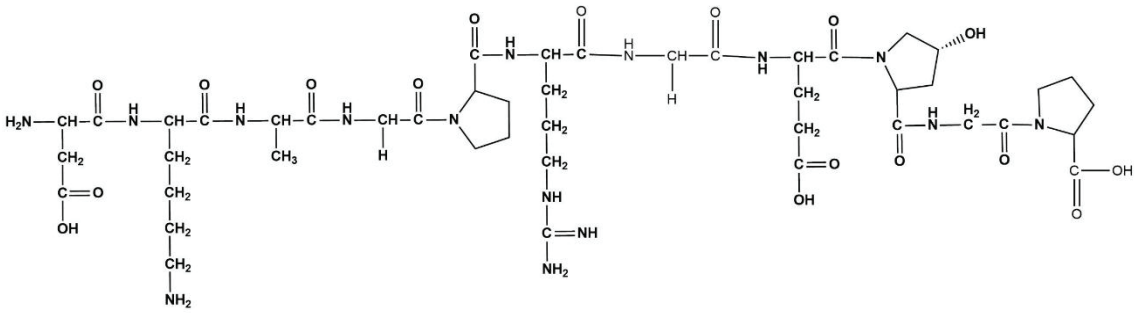

Asp - Lys - Ala - Gly - Pro - Arg - Gly - Glu - Hyp - Gly - Pro

Figure 1.5 The protein structure of gelatin and amino acids on the backbone.

CHAPTER 2

MATERIALS AND METHODS

2.1. Materials

Gelatin (Type A, 200 bloom from porcine skin), Methacrylic anhydride (MA), PBS (1x) and Dimethyl sulfoxide (DMSO), 2-Isocyanatoethyl methacrylate (Karenz, Sigma Aldrich) were utilized for modification of gelatin. 2-Hydroxy-4′-(2-hydroxyethoxy)-2-methylpropiophenone (Irgacure 2959, Sigma Aldrich), UltraPure water and UVP CL 1000 UV crosslinker with 365 nm wavelength tubes were used for fabrication of hydrogels. NIH 3T3 mouse fibroblast cells, DMEM (GIBCO, Thermo Fischer Scientific), L-glutamin and RPMI medium (GIBCO, ThermoFischer Scientific), penicillin/streptomycin, CytoCalcein™ Green and Propidium Iodide (PI) dyes (AATBioquest) and Alamar blue solution were used for cell culture experiments on hydrogels.

2.2. Methods

To synthesize hydrogels of GelMA and GelatinK gelatin is modified with methacrylic anhydride and 2-isocyanatoethyl methacrylate respectively. The modified gelatin were characterized by FT-IR spectroscopy. The hydrogels are synthesized and investigated in terms of morphology, swelling ratio and biocompatibility.

2.2.1. Modification of Gelatin with Methacrylic Anhydride (MA)

Gelatin was modified with methacrylic anhydride with different modification degrees using the procedure [140] with minor changes. The modification process is represented in Figure 2.1. Basically, 1 g gelatin was weighed and taken into round bottom flask with a stir bar. 10 ml of ultrapure water were added to a flask. The solution was mixed at 45 °C for 10-30 min until complete dissolution of gelatin. While stirring, slowly add methacrylic anhydride with the amount as shown in Table 2.1. If mixing is sufficient, the reaction solution will turn homogeneously opaque with the dispersion of methacrylic

anhydride in solution. The reaction was allowed to proceed for 3 hours at 45 °C under nitrogen atmosphere. To stop reaction, synthesis solution was diluted with three volumes of preheated (45 °C) UltraPure water. The resultant solution was put into -80 °C and freezed for several hours. After that, the frozen reaction solution was put into freeze-dryer to lyophilize until the polymer was fully dehydrated (2-3 days). The produced polymer was named as Gelatin methacryloyl, GelMA as shortly, and GelMA1, GelMA2, GelMA3, GelMA4 and GelMA5 according to modification degree of gelatin with MA. Lyophilized GelMA was stored at -80 °C to protect from light and moisture until use.

Table 2.1 Synthesis of GelMA with varying amount of MA.

GelMA	GelMA1	GelMA2	GelMA3	GelMA4	GelMA5
MA(ml/ 1g gelatin)	0.1	0.2	0.4	0.6	0.8

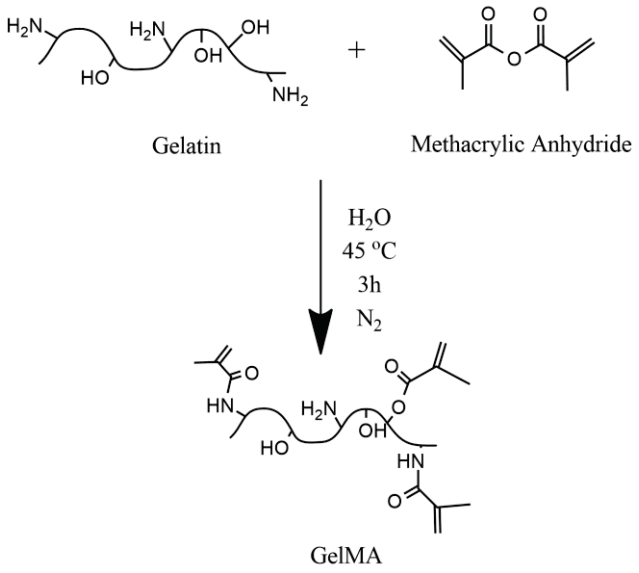

Figure 2.1 Modification of gelatin with methacrylic anhydride.

2.2.2. Modification of Gelatin with 2-Isocyanatoethyl Methacrylate

Gelatin was modified with 2-isocyanatoethyl methacrylate with different modification degrees using the procedure [141] by changing dextran with gelatin and allyl isocyanate with 2-isocyanatoethyl methacrylate without using a catalyst. The modification process of gelatin is represented in Figure 2.2. Basically, 1 g gelatin was weighed and taken into round bottom flask with a stir bar. 27 ml of DMSO is added to the flask. The solution was mixed at 50 °C for 30-40 min until complete dissolution of

gelatin. While stirring, slowly add 2-isocyanatoethyl methacrylate with the amount as shown in Table 2.2. The reaction was allowed to proceed for 6 hours at 50 °C under nitrogen atmosphere. The white solid product was precipitated with addition of excess amount of cold isopropanol to reaction solution. This solution was centrifuged at 2500 rpm for 5 min at RT. Gelatin-urea solid product was decanted into a large glass beaker by pipetting solvent phase at top of the solid. The white solid was freezed at -80 °C for several hours. After that, the frozen solid was put into freeze-dryer to lyophilize until the Gelatin-urethane was fully dehydrated (2-3 days). The produced Gelatin-Urethane polymer are named as GelatinK1, Gelatink2, GelatinK3, GelatinK4 and GelatinK5 according to modification degree of gelatin with Karenz. The lyophilized polymer is stored at –80 °C to protect from light and moisture until use.

Table 2.2 Synthesis of Gelatin-Urethane with varying amount of Karenz.

Gelatin-Urethane	GelatinK1	GelatinK2	GelatinK3	GelatinK4	GelatinK5
Karenz(µl/ 1g gelatin)	74.6	149.2	268.6	388	448

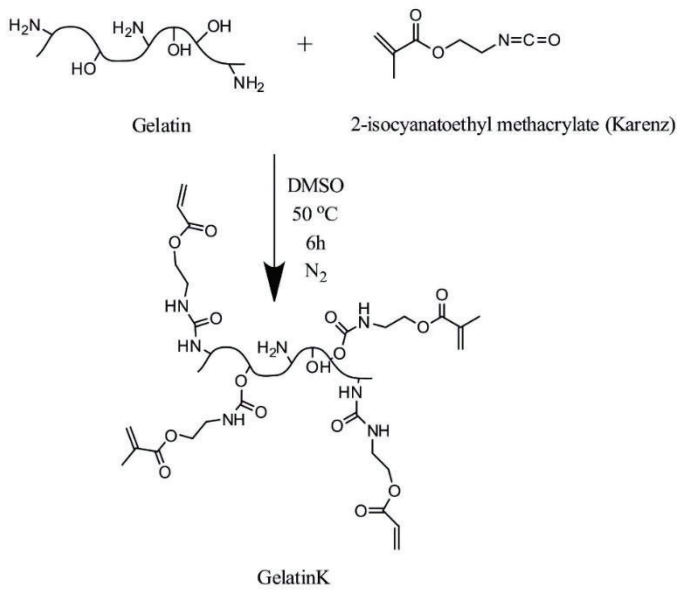

Figure 2.2 Modification of gelatin with 2-Isocyanatoethyl methacrylate (Karenz) to obtain GelatinK polymer.

2.2.3. Synthesis of Hydrogels

Hydrogels of GelMA and GelatinK were synthesized by photopolymerization reaction. The schematic of gelation process of GelatinK and GelMA is demonstrated in Figure 2.3. The redox initiator was chosen as Irgacure 2959. Irgacure 2959 was dissolved in ultrapure water to final concentration of 1% (w/v) by heating to 50 °C. Then, GelMA or GelatinK polymer was dissolved in Irgacure solution at 50 °C at final concentrations 5, 7.5, 10 and 15% (w/v). After complete dissolution of polymer in Irgacure, polymer was taken into 1 ml syringe and put into UV cabinet for gelation. The gelation time was determined by controlling the polymer solution at 60 sec arrivals. The gelation time for GelMA hydrogel was 5 min while it was 2 min for GelatinK hydrogel.

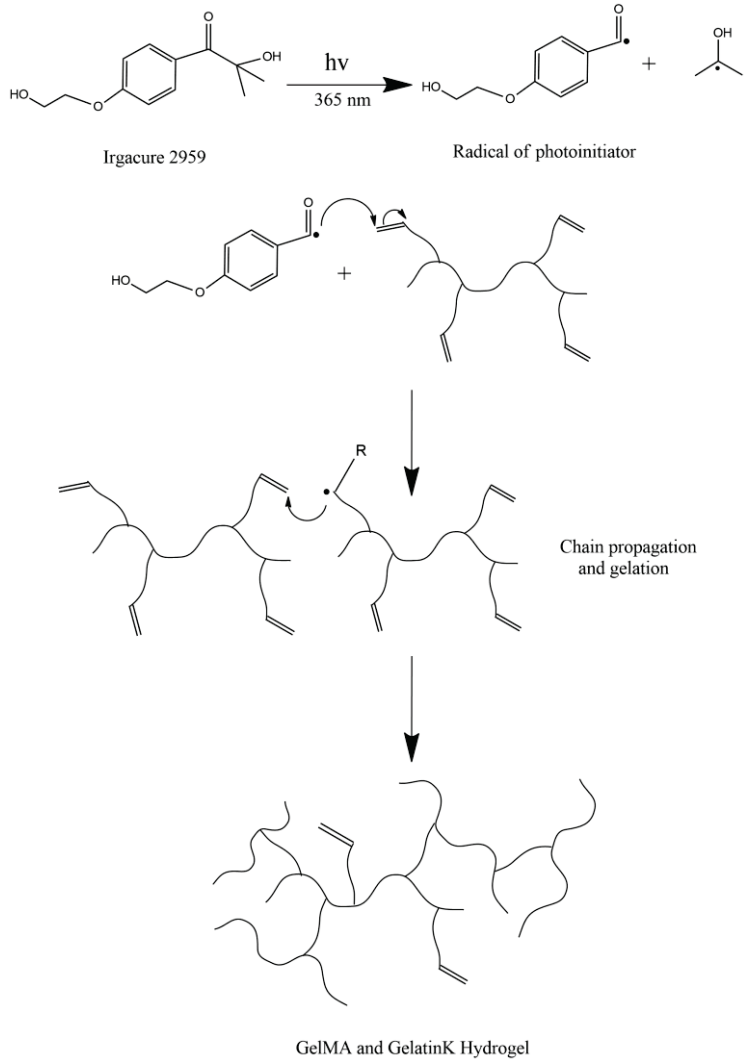

Figure 2.3 Gelation of GelatinK and GelMA polymer in the presence of redox initiator under UV curing.

2.2.4. Characterization Experiments

GelMA and GelatinK polymers and their hydrogels are characterized with FT-IR spectroscopy, SEM imaging, swelling experiments and cell culture experiments.

2.2.4.1. Fourier Transform Infrared - Attenuated Total Reflectance Spectroscopy (FTIR-ATR) Analysis

GelMA and GelatinK polymers were freeze-dried to remove solvent for ATR analysis. This analysis was performed to investigate the modification of gelatin. Spectrums of freeze-dried polymers were taken using FTIR-ATR instrument with diamond/ZnSe crystal (Perkin Elmer-UATR TWO). The analysis was conducted between 650 - 4000 cm^{-1} wavenumber range with a resolution rate of 4 cm^{-1} and scan number of 20. The obtained data were plotted using graphing software OriginPro (Northampton, MA).

2.2.4.2. SEM Analysis of Hydrogels

To characterize morphology, hydrogels were frozen at –80 °C and freeze-dried after synthesis to remove water absorbed within a gel. The dried samples were cut into fragments, fixed on carbon bands and coated with a thin gold layer under argon gas (Emitech K550X). The samples were observed by scanning electron microscopy (FEI Quanta 250 FEG (Oregon, USA)) in varied magnifications. The pore size of the hydrogels was determined using ImageJ Software (NIH) by averaging data from at least 100 points on the surface. Figure 2.4(A) shows the SEM image of GelMA1 5% (w/v) hydrogel and measuring pore size with ImageJ software using yellow straight line. In Figure 2.4(B) histogram of measured pore size values are shown. The statistics of this measurement is seen in Figure 2.4(C). The mean value in the statistics are the average pore size of the hydrogel.

2.2.4.3. Swelling Measurements

The swelling ratio (SR) of hydrogels were analyzed using freeze-dried gel samples to investigate water absorption capacity. Hydrogel pieces were freeze-dried after synthesis and the dry weight of gels was recorded (W_{dry}).

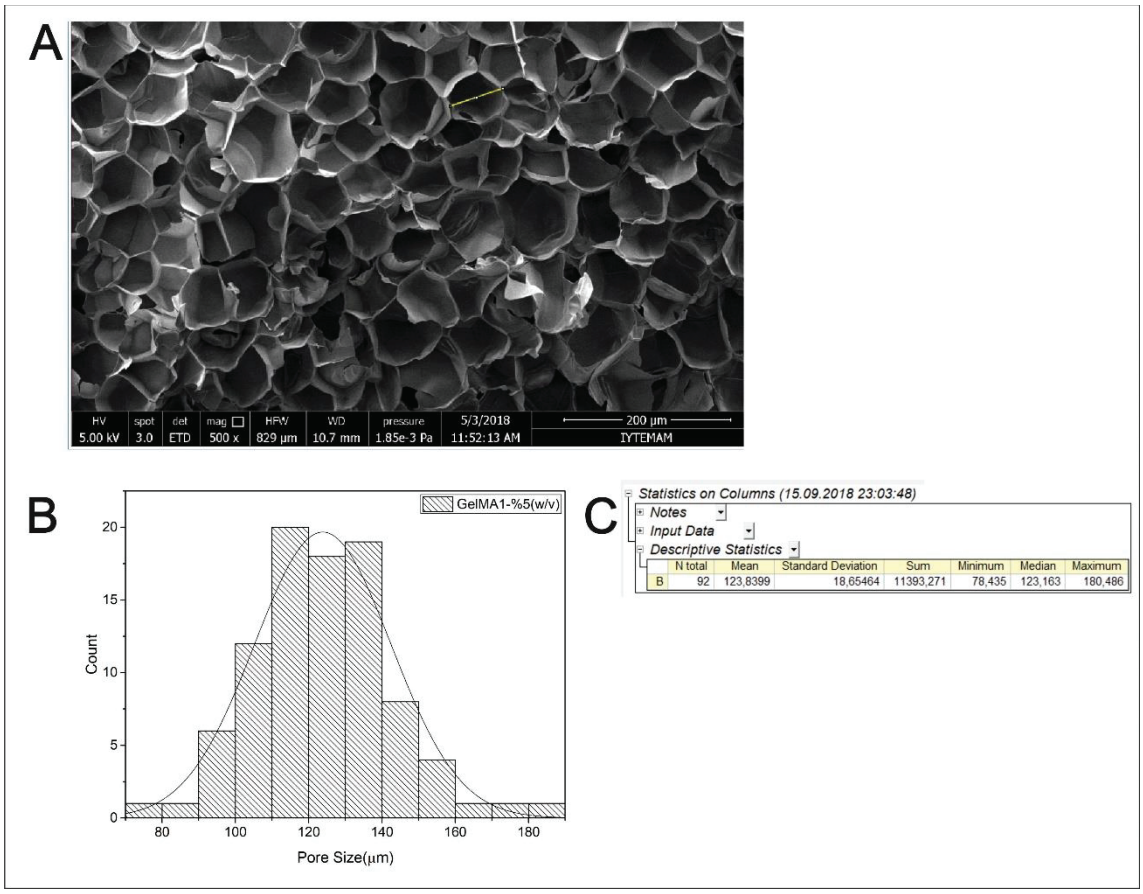

Figure 2.4 Determination of pore size of hydrogels. a) Pore sizes are measured with yellow straight line, b) Histogram of pore size distribution of the hydrogel sample, c) Statistics of the histogram showing mean of pore size.

They were put into distilled water in a storage container. Samples were taken out after every 24 h, excess water on the surface was absorbed with tissue paper and then swollen weight of hydrogel sample was measured. The formula to calculate the percent swelling ratio (% SR) is given in equation 2.1.

$$\%SR = \left(\frac{W_{swollen} - W_{dry}}{W_{dry}}\right) \text{x} 100 \qquad (2.1)$$

%SR is the percent swelling ratio, $W_{swollen}$ is weight of hydrogel after swelling in water, W_{dry} is the dry weight of hydrogel before immersing to water.

2.2.4.4. Cell Viability Experiments

NIH 3T3 mouse fibroblast cells were cultured in high glucose DMEM (GIBCO, Thermo Fischer Scientific) containing L-glutamine, supplemented with 1% penicillin/streptomycin and 10% Fetal Bovine Serum (GIBCO, Thermo Fischer Scientific). The cells were cultured up to ~90% confluency in a humidified environment (5% CO_2, 37 °C). The harvested cells were used further for cell viability studies. GelMA and GelatinK hydrogels were prepared with the same procedure as mentioned before. Here, 40 µl polymer solution were dropped into well in a 96 well plate. All concentrations of polymer solution was dropped with the same amount into a different well. The hydrogels were prepared with three repetitions. After that, the 96 well plate was put into UV cabinet for gelation. 10000 cell/well was used in this assay. After, the prepared well plate was incubated for 24 hours in a humidified environment (5% CO_2, 37 °C).

In Alamar Blue assay experiments, Alamar blue solution was added to each well and final concentration of Alamar blue solution was 0.01% in 100 µl. All the concentrations and the control group were evaluated from 3 samples. After 2-4 h incubation, analysis was carried out at the wavelength of 570 and 600 nm using by Multiskan™ GO Microplate Spectrophotometer (Thermo Fischer Scientific).

CHAPTER 3

RESULTS AND DISCUSSION

3.1. Synthesis of GelMA and GelatinK Polymers

GelMA and GelatinK polymers were produced by modification of gelatin with varying amounts of MA and Karenz respectively. The images of lyophilized polymers are shown in Figure 3.1. Images of freeze-dried GelatinK4 and GelatinK5 are shown in Figure 3.2. They are film-like hard and brittle materials which are not suitable to analyze since the handling of these hard samples is difficult. Also, GelatinK4 and GelatinK5 are not soluble in water so polymerization could not be carried with these two polymers.

Figure 3.1 Images of GelMA and GelatinK polymers after lyophilization.

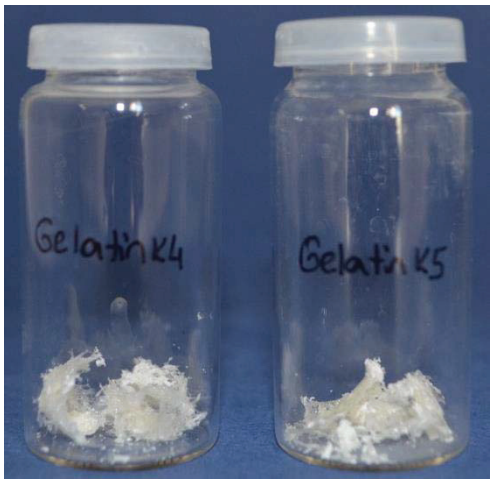

Figure 3.2 Images of GelatinK4 and GelatinK5 after lyophilization process.

3.2. FTIR-ATR Characterization of GelMA and GelatinK Polymers

Gelatin was modified with methacrylic anhydride and Karenz. The produced GelMA and GelatinK polymers were characterized by FTIR spectroscopy. The FTIR spectrum of gelatin is shown in Figure 3.3. Amide I, amide II and amide III bands appear at 1633, 1526 and 1236 cm^{-1} respectively. The amide I vibration mode attributes to C=O stretching vibration coupled to contributions from the C-N stretch, CCN deformation and in-plane N-H bending modes [142]. The absorption at amide I vibration is characteristic for the coil structure of gelatin [143]. Amide II band occurs due to the bending vibration of N-H groups and stretching vibrations of C-N groups. Also, amide III band is seen in case of loss of α helix structure of gelatin with vibrations of C-N stretching and N-H bending of amide bond. The signal at 3282 cm^{-1} is responsible for N-H stretching vibration coupled with hydrogen bonding and O-H stretching of hydrogen bonded hydroxyl groups. The signal at 3072 cm^{-1} corresponds to C-H stretching while 2938 cm^{-1} corresponds to asymmetric stretching vibration of =C-H and also NH_3^+. C=O bending vibration gives a signal at 1335 cm^{-1} as seen in Figure 3.3.

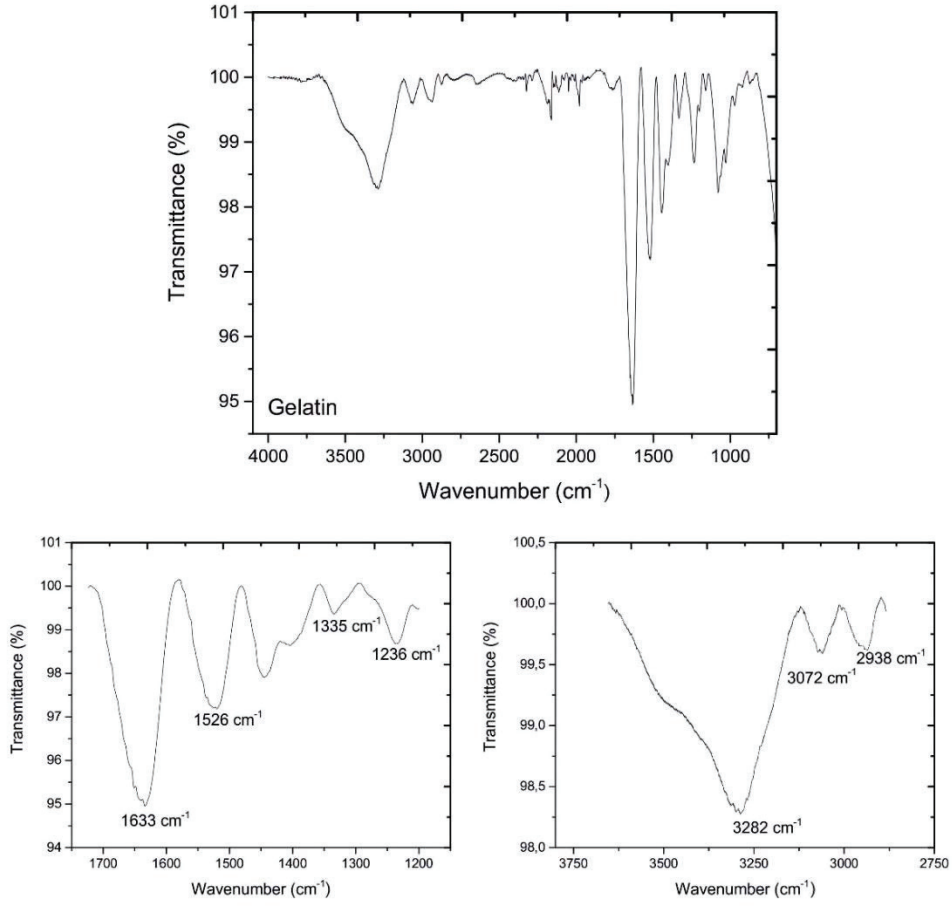

Figure 3.3 FTIR spectra of pure gelatin.

Figure 3.4 shows the FTIR spectra of pure gelatin and five GelMA polymers. The main amide I, amide II and amide III bands in GelMA polymers are as the same as in pure gelatin. If the spectra is investigated closely, the specific bands are become clear in GelMA polymers. C-H stretching of C=C bonds of methacrylate group gives two specific signals at 943 cm^{-1} and 863 cm^{-1} as seen in Figure 3.5(A). Also, the signal at 1652 cm^{-1} appears in all GelMA formulations representing C=C stretching in methacrylate groups on backbone due to methacrylation of gelatin (Figure 3.5(B)). These three signals are become more intensive from GelMA1 to GelMA5, except GelMA4, since methacrylation degree increases towards GelMA5 polymer as clearly explained in Table 2.1. All in all, when the spectra of pure gelatin and GelMA polymers are investigated in detail, it can be understood that gelatin was modified with methacrylic anhydride with different modification degrees in GelMA polymers.

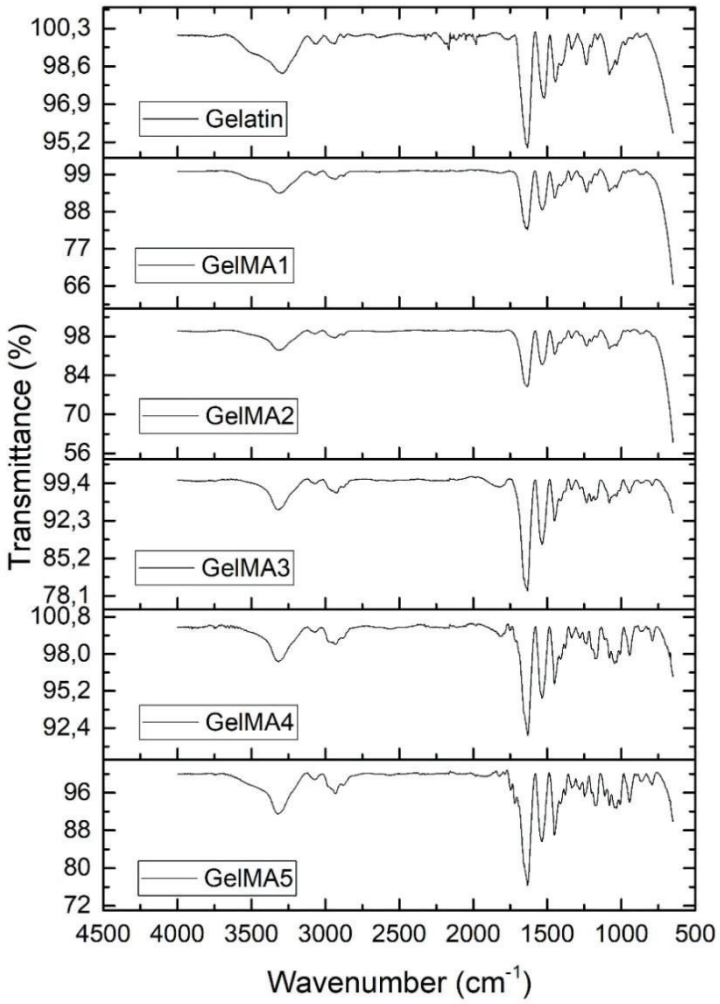

Figure 3.4 FTIR spectra of pure Gelatin and GelMA polymers.

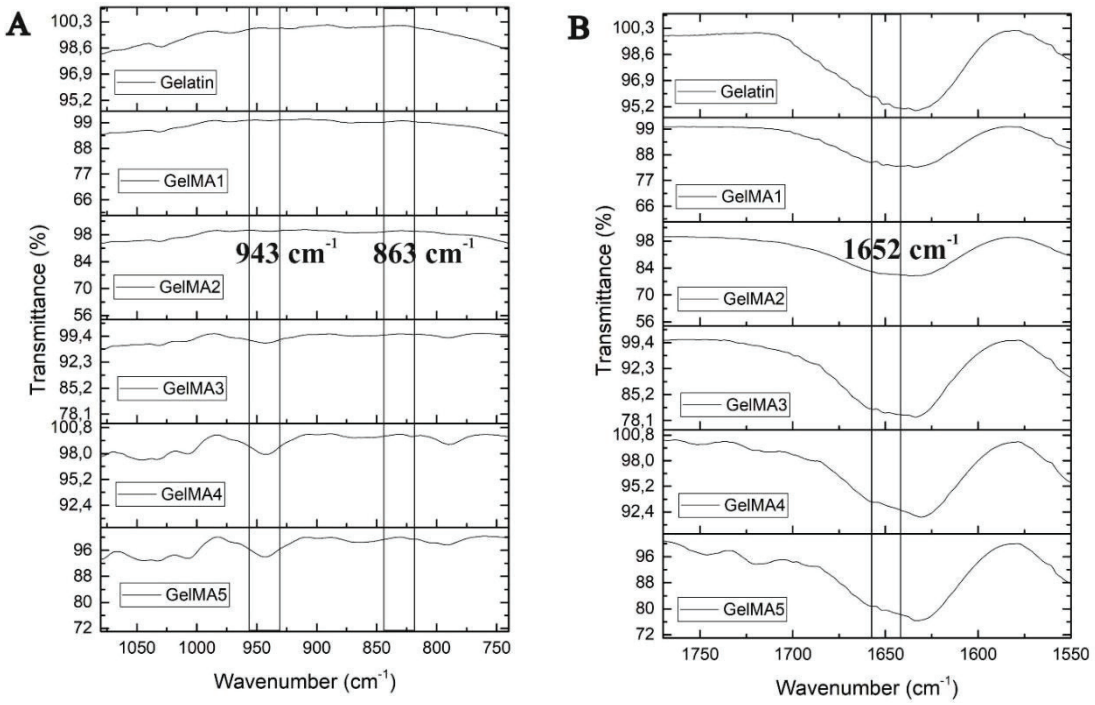

Figure 3.5 FTIR spectra of pure Gelatin and GelMA polymers. a) Between 1080-740 cm^{-1}, b) Between 1770-1550 cm^{-1} wavenumbers.

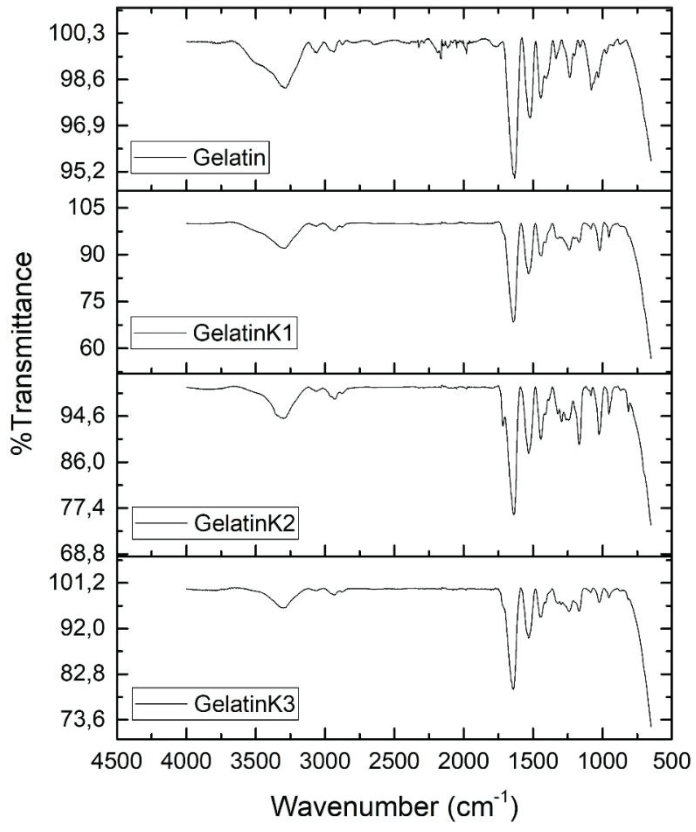

Figure 3.6 FT-IR spectra of pure Gelatin and GelatinK polymers.

Moreover, modification of gelatin with Karenz contributes to significant changes in the spectrum of gelatin. Figure 3.6 demonstrates the spectra of pure gelatin and GelatinK polymers. As seen in Figure 3.6, the main amide I, amide II and amide III bands did not change with modification. However, four important bands are present in spectrum of GelatinK polymers but not in pure gelatin when Figure 3.7 is investigated in detail. C=O stretching vibration band of urea and urethane carbonyl groups located at 1718 cm^{-1} (Figure 3.7 (a)). Another bands at 1166, 953 and 813 cm^{-1} contribute to carbonyl C-O stretching of carbonyl group, =C-H stretching and C=C stretching respectively (Figure 3.7(b)).

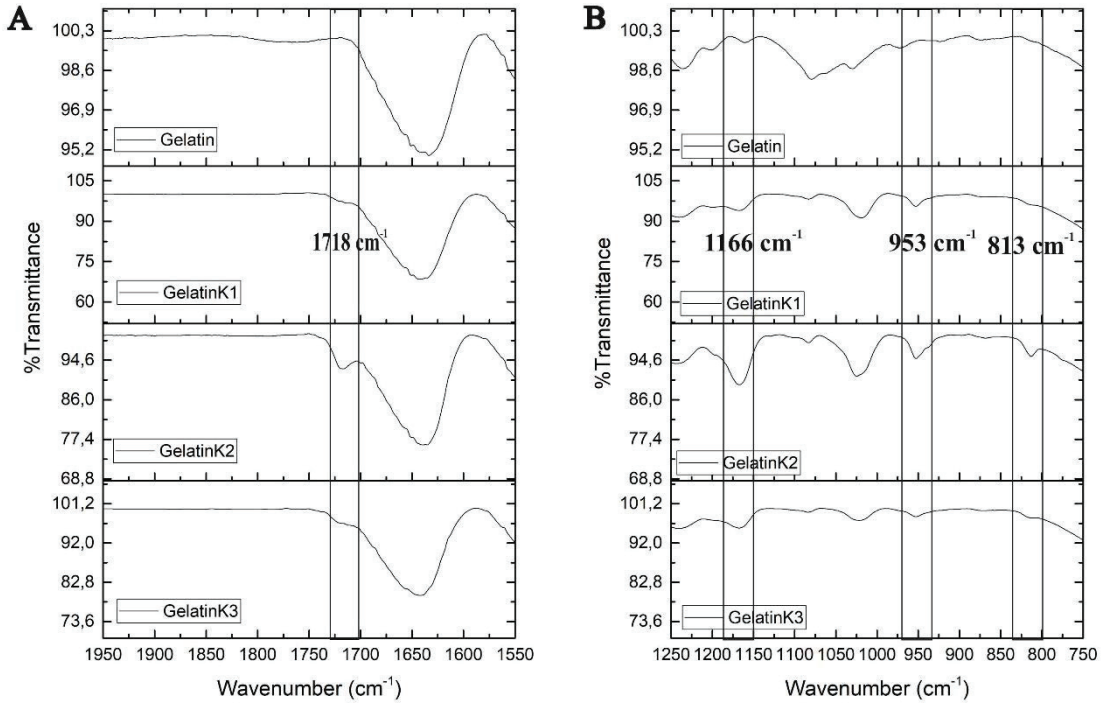

Figure 3.7 FTIR spectra of pure Gelatin and GelatinK polymers. a) Between 1950-1550 cm^{-1}, b) Between 1250-750 cm^{-1} wavenumbers.

3.3. Synthesis of Hydrogels

GelMA and GelatinK hydrogels were synthesized in 1% Irgacure solution by photopolymerization under UV curing. The images of hydrogels can be seen in the Figure 3.8. Figure 3.8 (a) demonstrate GelMA hydrogels after synthesis, after freeze-drying and after swelling in water respectively. In Figure 3.8(b) GelatinK hydrogels are shown Freeze-dried samples are soft and easy to cut for both GelMA and GelatinK hydrogels. When hydrogels are immersed in water, they absorb high amount of water.

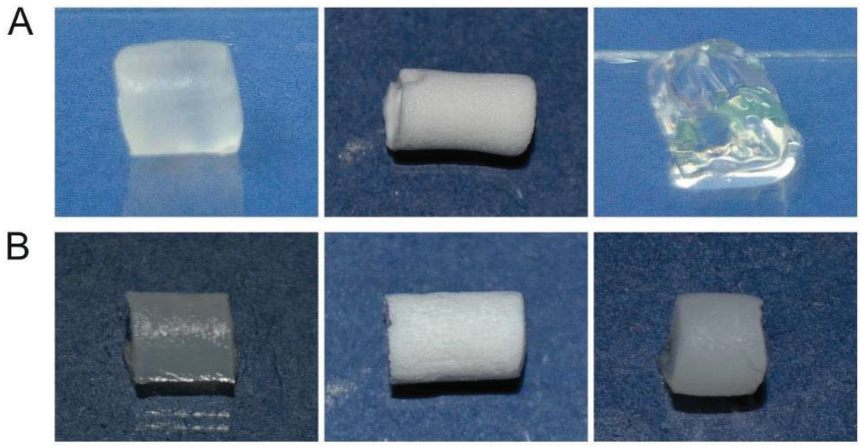

Figure 3.8 Hydrogel images of; a) GelMA, b) GelatinK. Images represents hydrogels after synthesis, after freeze-drying process and after swelling in water respectively.

3.4. SEM Analysis of Hydrogels

SEM images of freeze-dried hydrogels were taken to investigate the morphology and porosity of surface of the materials. SEM images of GelMA hydrogels are shown in Figure 3.9, Figure 3.10, Figure 3.11, Figure 3.12 and Figure 3.13. As seen in SEM images, all GelMA hydrogels are porous but pore sizes are different for not only GelMA formulations but also polymer concentration. The image of whole gel is uniformly porous like in %5 GelMA2 (Figure 3.10(a)). Pores are not uniform in some hydrogel samples, this may be a result of freeze-drying process. Also, pore sizes (μm) of GelMA hydrogels are seen in Figure 3.14. Pore sizes of GelMA hydrogels decrease as methacrylation degree of gelatin increases regardless of the polymer concentration. For example, 5% (w/v) GelMA1 has almost 124 μm pores while GelMA5 has nearly 14 μm (Figure 3.14 (a)). Pore size of GelMA1 and GelMA5 are 95 μm and 21 μm respectively in 10% (w/v) gels. Also, as can be seen in Figure 3.15, when polymer concentration enhanced from 5% to 15%, average pore size declined in all polymer formulations. In GelMA4, pore size decrease from nearly 74 μm to 9 μm when going from 5% to 15% (w/v) polymer concentration. Also in GelMA2, 5% gel has nearly 69 μm while 15% gel has 13 μm pore. The same tendency to decrease in pore size are seen in all GelMA formulations.

Pore wall lengths of hydrogels were also calculated. Figure 3.16 shows the pore wall size distributions of GelMA1 and GelMA2 hydrogels in 5 and 15% concentrations. Pore walls in GelMA1 hydrogel were calculated as 8 and 1.2 μm in 5% and 15% concentrations Figure 3.16(a, b).

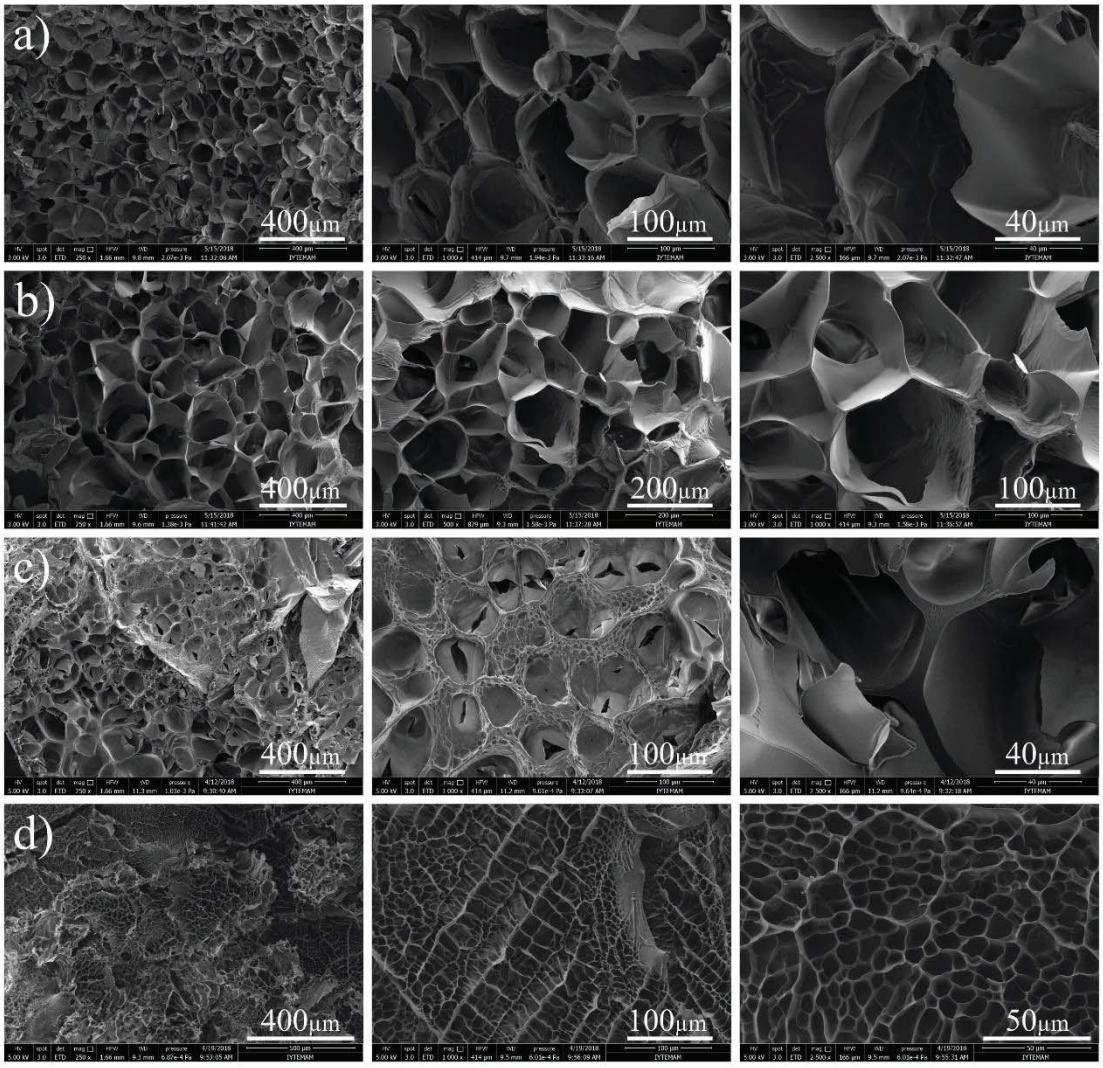

Figure 3.9 SEM images of GelMA1 hydrogels in different polymer concentrations. a) 5% (w/v), b) 7.5% (w/v), c) 10% (w/v), d)15% (w/v).

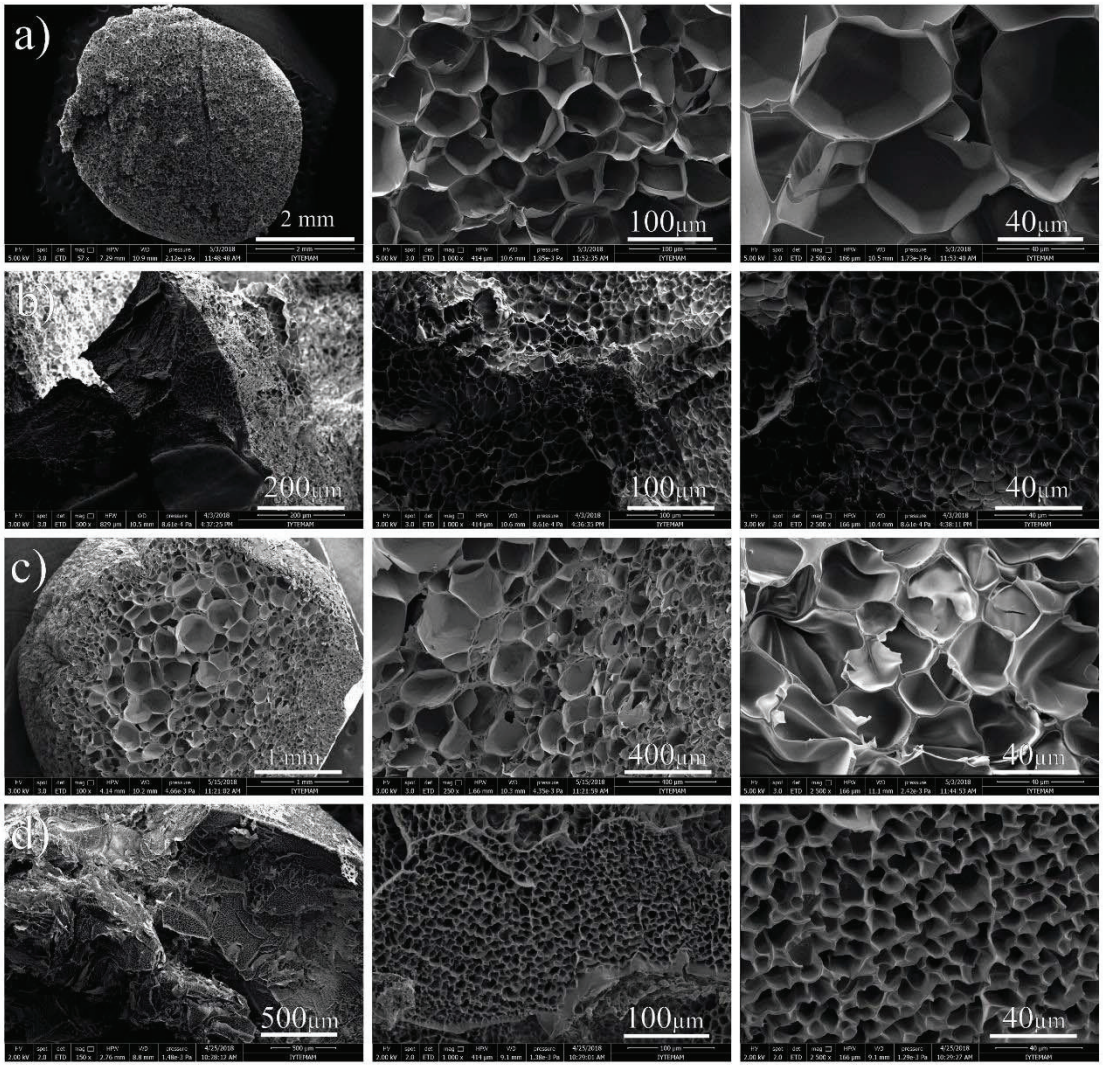

Figure 3.10 SEM images of GelMA2 hydrogels in different polymer concentrations. a) 5% (w/v), b) 7.5% (w/v), c) 10% (w/v), d)15% (w/v).

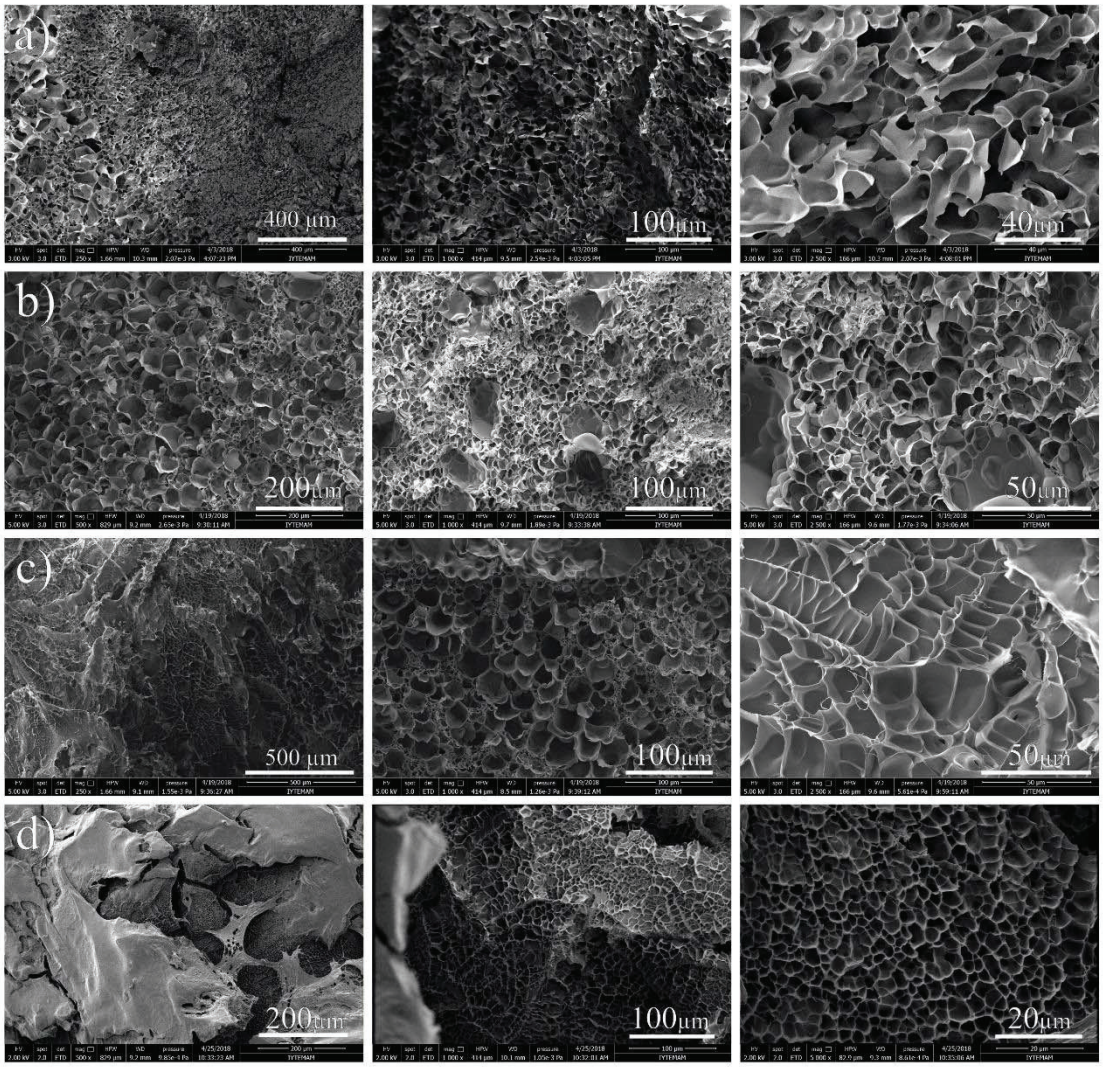

Figure 3.11 SEM images of GelMA3 hydrogels in different polymer concentrations. a) 5% (w/v), b) 7.5% (w/v), c) 10% (w/v), d) 15% (w/v).

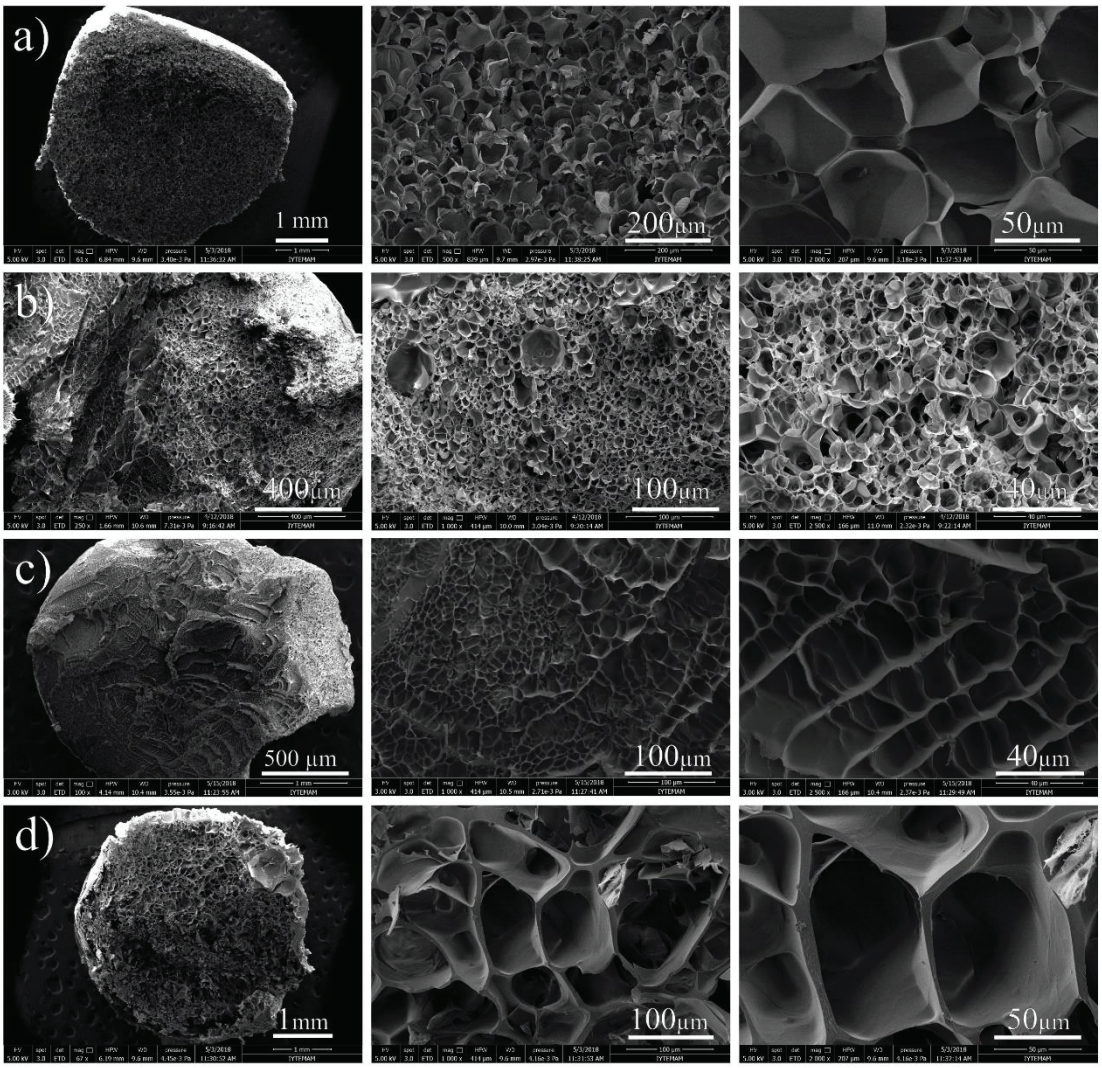

Figure 3.12 SEM images of GelMA4 hydrogels in different polymer concentrations. a) 5% (w/v), b) 7.5% (w/v), c) 10% (w/v), d) 15% (w/v).

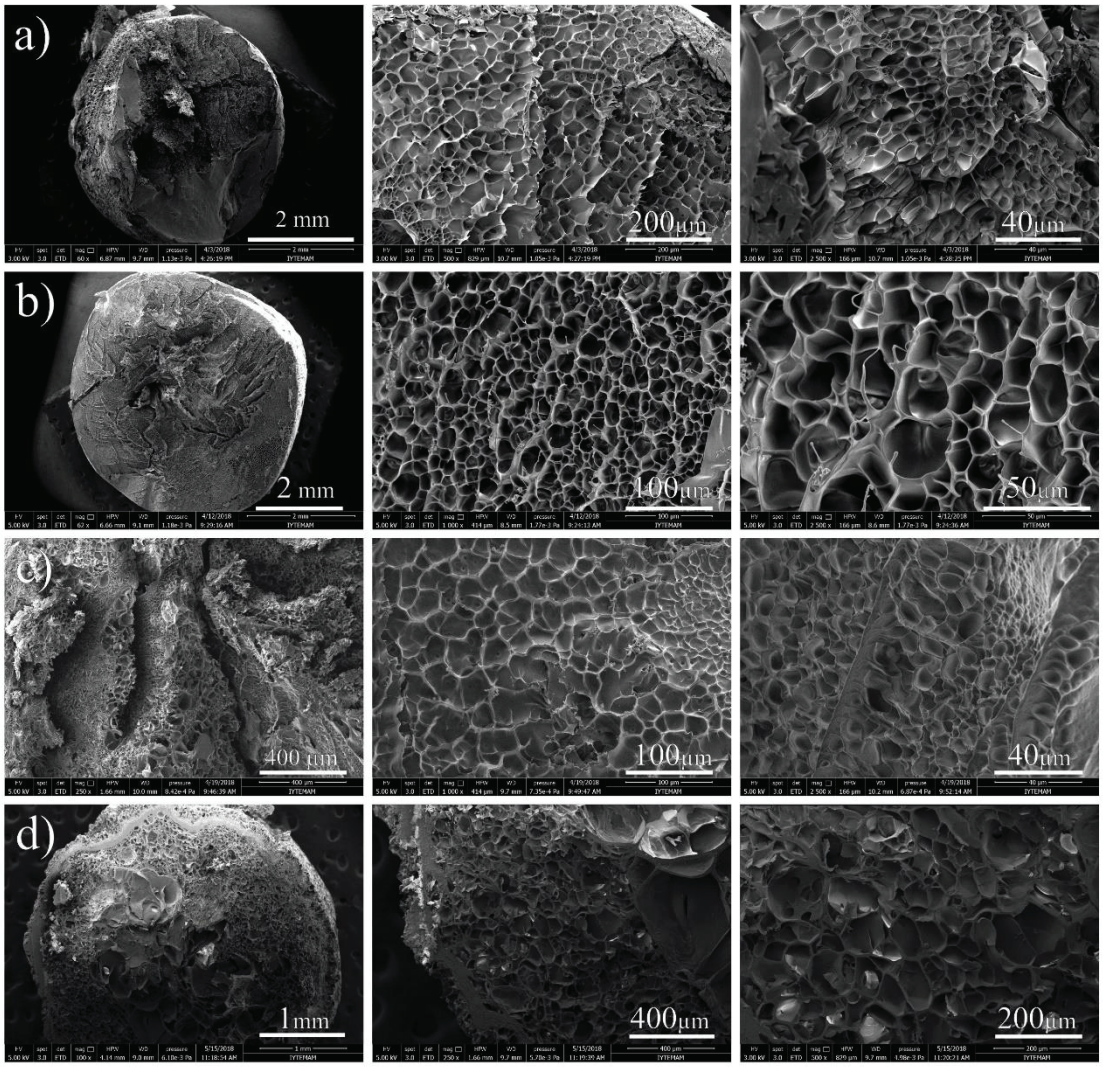

Figure 3.13 SEM images of GelMA5 hydrogels in different polymer concentrations. a) 5% (w/v), b) 7.5% (w/v), c) 10% (w/v), d) 15% (w/v).

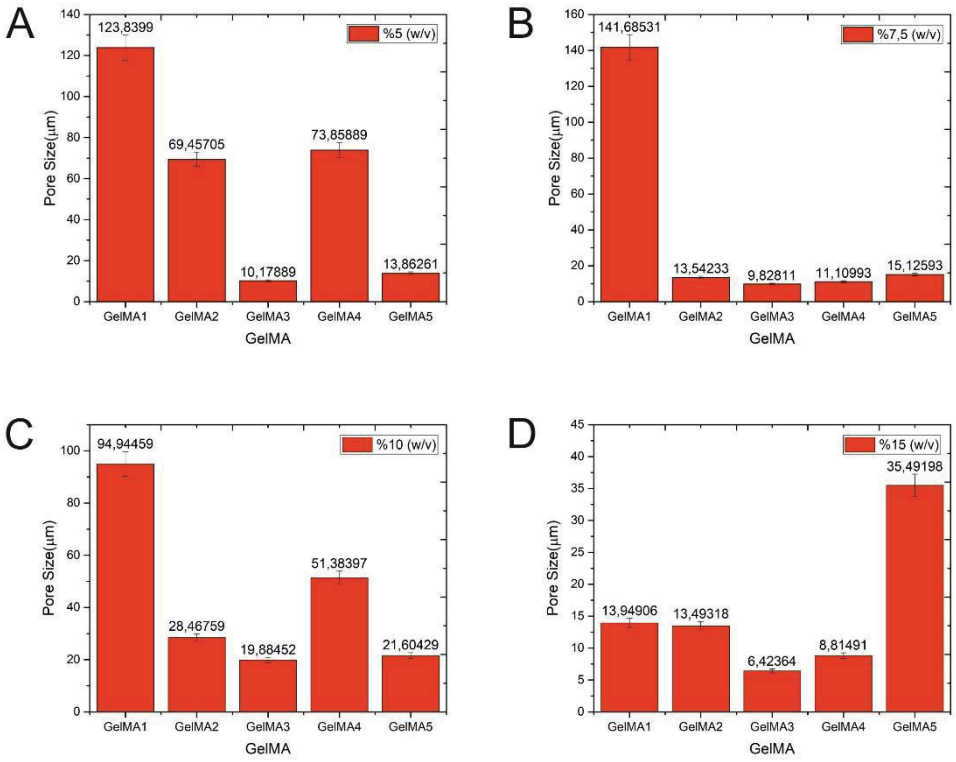

Figure 3.14 Pore sizes (µm) of GelMA hydrogels with concentration of; a) 5% (w/v), b) 7.5% (w/v), c) 10% (w/v), d) 15% (w/v) GelMA polymer.

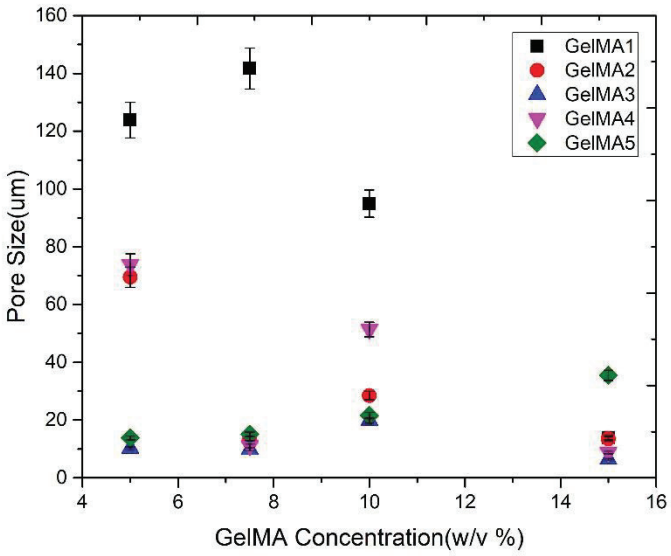

Figure 3.15 Pore sizes (µm) of GelMA1, GelMA2, GelMA3, GelMA4 and GelMA5 hydrogels.

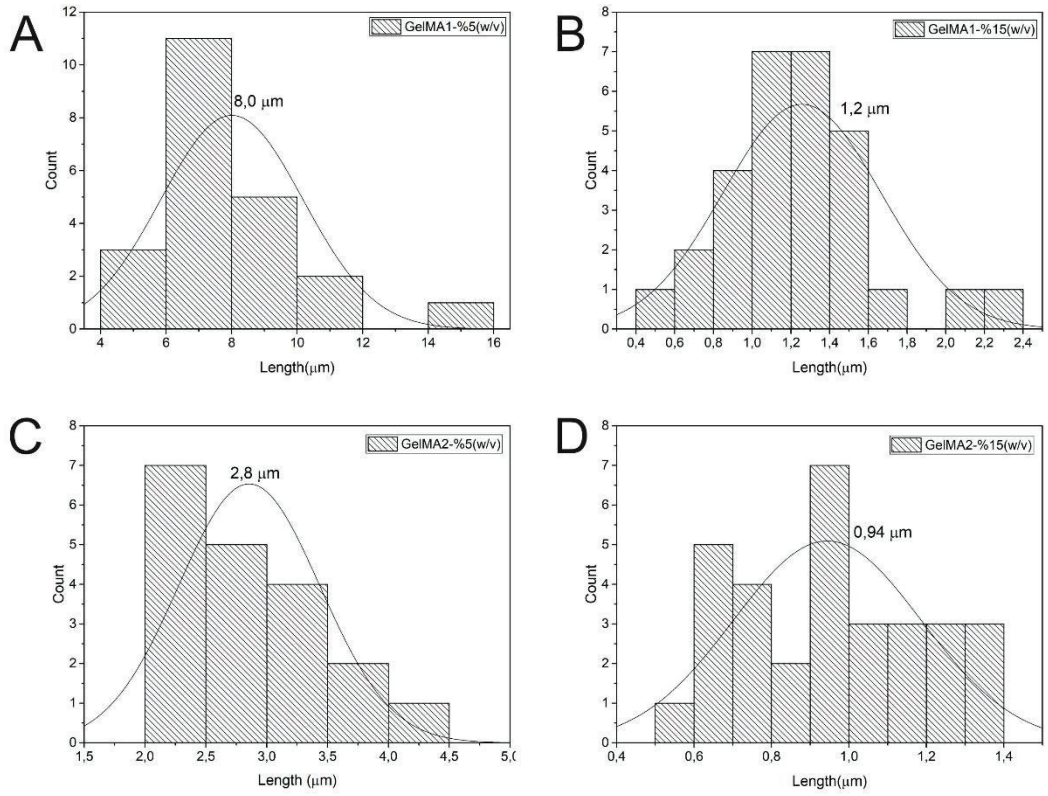

Figure 3.16 Pore wall lengths (μm) of GelMA hydrogels. a) GelMA1 5% (w/v), b) GelMA1 15% (w/v), c) GelMA2 5% (w/v), d) GelMA2 15% (w/v).

GelMA2 hydrogels have 2.8 and 0.94 μm pore walls in 5% and 15% hydrogels as shown in Figure 3.16(c, d). It can be said that pore walls of hydrogels may get thinner when polymer concentration and methacrylation, also crosslinking, degree increases.

SEM images of GelatinK hydrogels are also investigated with freeze-dried samples. Figure 3.17, Figure 3.18 and Figure 3.19 show the SEM image of GelatinK1, GelatinK2 and GelatinK3 respectively. As seen, all hydrogels with different formulations and polymer concentrations are porous with different pore sizes (μm). 5% (w/v) gel in GelatinK3 has nonhomogeneous morphology as seen in Figure 3.19(a). However, other hydrogel samples show high porous morphology. The samples were examined from 1mm or 2mm distance firstly to see whole surface of hydrogel as in Figure 3.17(a, b), Figure 3.18(b, d) and Figure 3.19 (a, b, c, and d). From this distance, surface of whole sample is porous with clear pores.

Figure 3.20 and Figure 3.21 demonstrate trend in pore sizes of hydrogel formulations. As seen, pore size decreases from GelatinK1 to GelatinK3. For example, GelatinK1, GelatinK2 and GelatinK3 hydrogels have nearly 144, 124 and 99 μm pore

size in 7.5% (w/v) gel. The deviations in this trend are possibly due to experimental errors during synthesis and freeze-drying process of hydrogels. Sometimes, GelatinK polymer and hydrogels show deteriorations during freeze-drying procedure and this leads to solubility problem in GelatinK polymer and morphological damages in GelatinK hydrogels. Furthermore, it can be said that pore size of the hydrogels rise with increasing polymer concentration (Figure 3.21). For instance, GelatinK2 has almost 55, 124, 88 and 160 μm pore sizes in 5, 7.5, 10 and 15% (w/v) gels respectively. 5% and 15% (w/v) gels of GelatinK1 show almost 68 and 108 μm pores.

Pore wall lengths of GelatinK hydrogels were calculated. Figure 3.22 shows the pore wall size distributions of GelatinK1 and GelatinK2 hydrogels in 5% and 15% (w/v) polymer concentrations. GelatinK1 hydrogel has 4.15 μm and 7.86 μm pore walls in 5% and 15% (w/v) respectively. Whereas, pore walls in GelatinK2 hydrogels are 2.2 μm and 10.35 μm in 5% and 15% (w/v) respectively. According to these measurements, it can be said that pore wall lengths of GelatinK and GelMA hydrogels may change with not only modification degree and polymer concentrations. But measurements should be done for all hydrogel formulations.

3.5. Swelling Properties of Hydrogels

Freeze-dried hydrogel samples were weighted and immersed in distilled water to reach equilibrium swollen condition. The weight of samples were measured until the hydrogels reach constant weight. Then percent swelling ratios (%SR) of hydrogels were calculated using the formula in equation 2.1. %SR is the percent swelling ratio, $W_{swollen}$ is weight of hydrogel after swelling in water, W_{dry} is the dry weight of hydrogel before immersing to water.

Percent swelling ratio of hydrogels prepared with GelMA1, GelMA2, GelMA3, GelMA4 and GelMA5 with concentrations of 5%, 7.5% 10% and 15% (w/v) GelMA polymer are shown in Figure 3.23. As seen, %SR decreases from GelMA1 to GelMA5 in all GelMA concentrations due to increasing methacrylation degree. Methacrylation of gelatin proceeds through NH_2 and OH groups on gelatin backbone so the increasing MA on backbone decreases free amino groups. Amino groups are able to capture H^+ and polymer chains gets far from each other absorbing water into the gap between polymer chains and hydrogel swells in water.

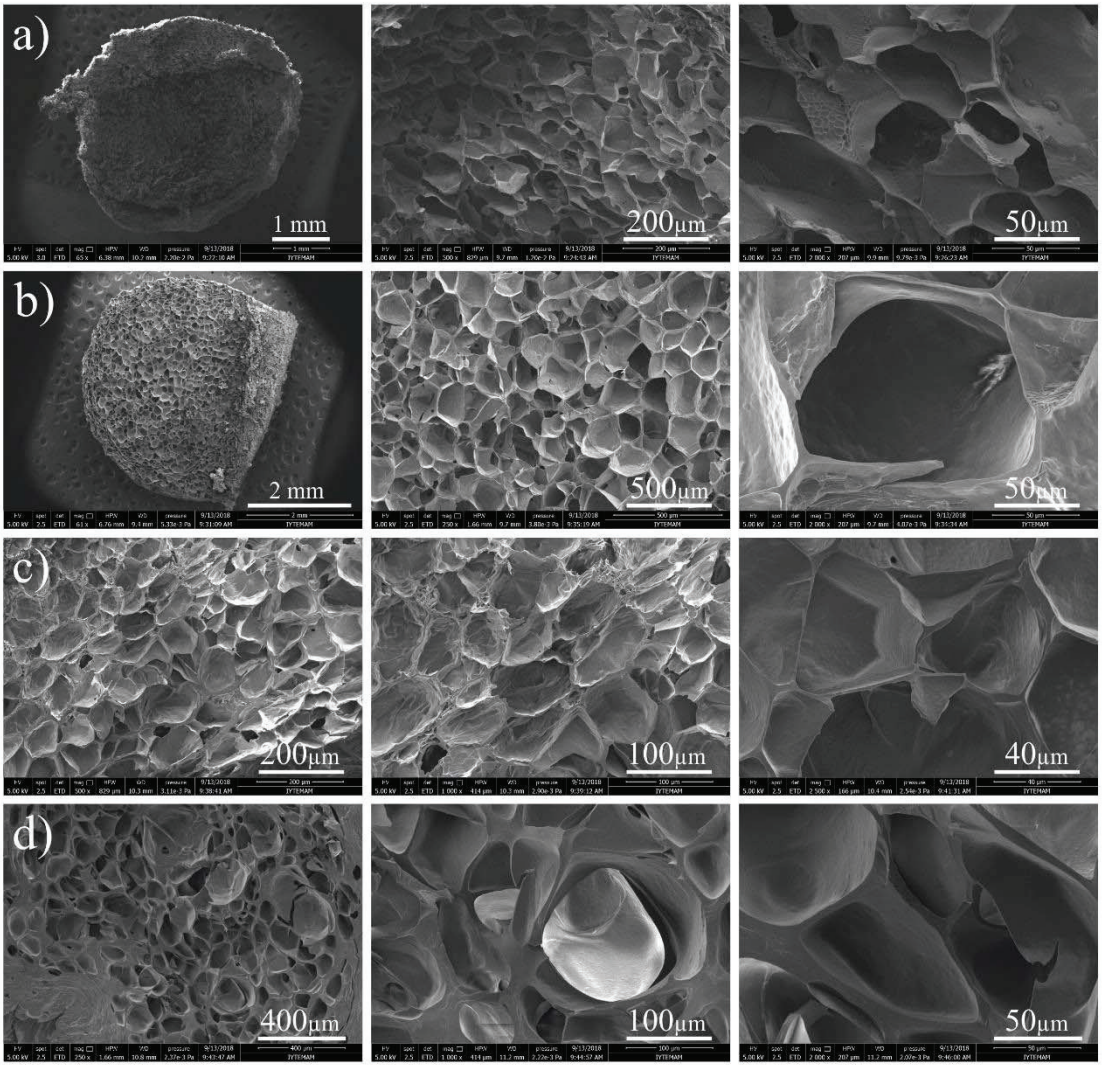

Figure 3.17 SEM images of GelatinK1 hydrogels in different polymer concentrations. a) 5% (w/v), b) 7.5% (w/v), c) 10% (w/v), d) 15% (w/v).

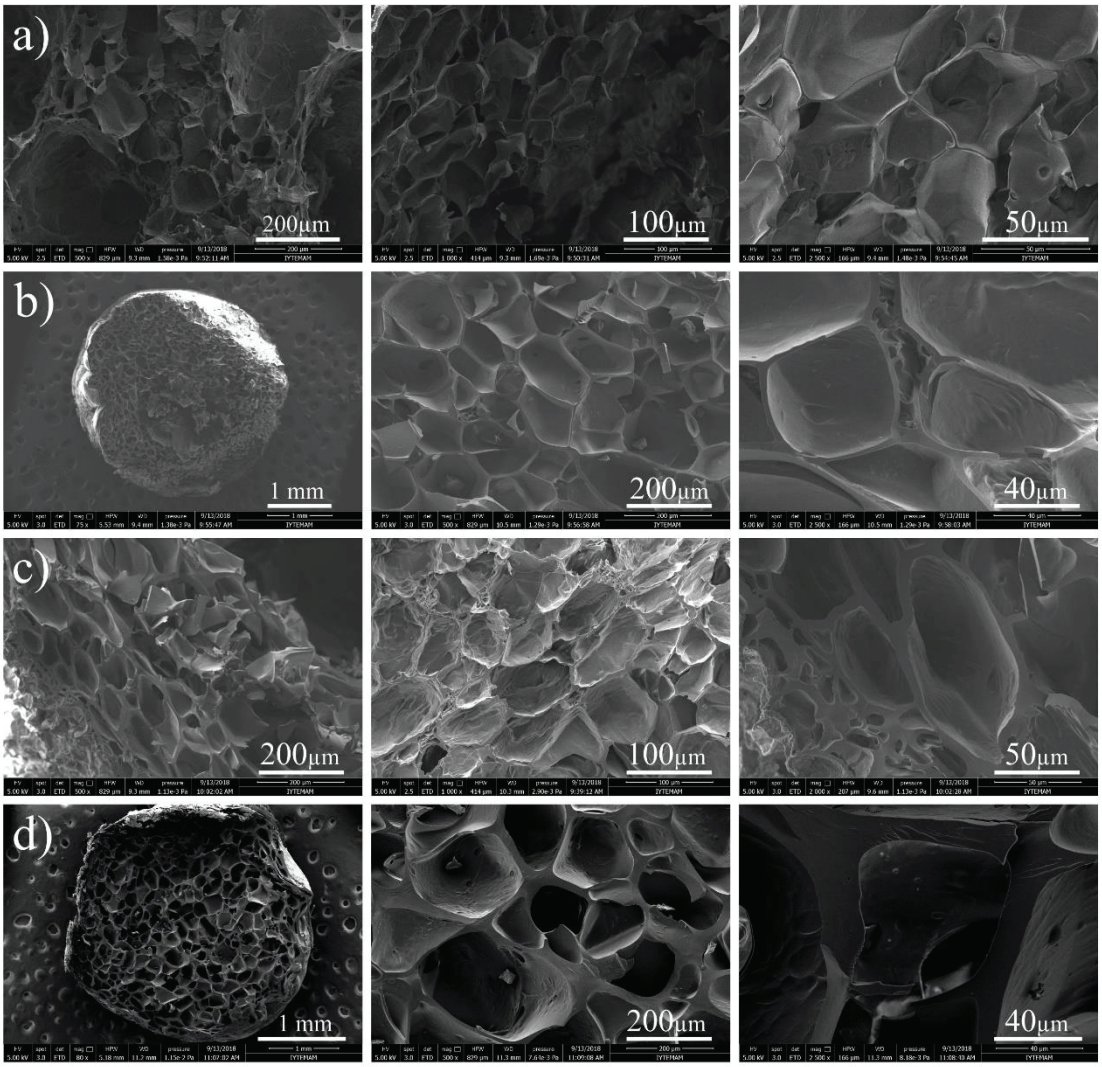

Figure 3.18 SEM images of GelatinK2 hydrogels in different polymer concentrations. a) 5% (w/v), b) 7.5% (w/v), c) 10% (w/v), d) 15% (w/v).

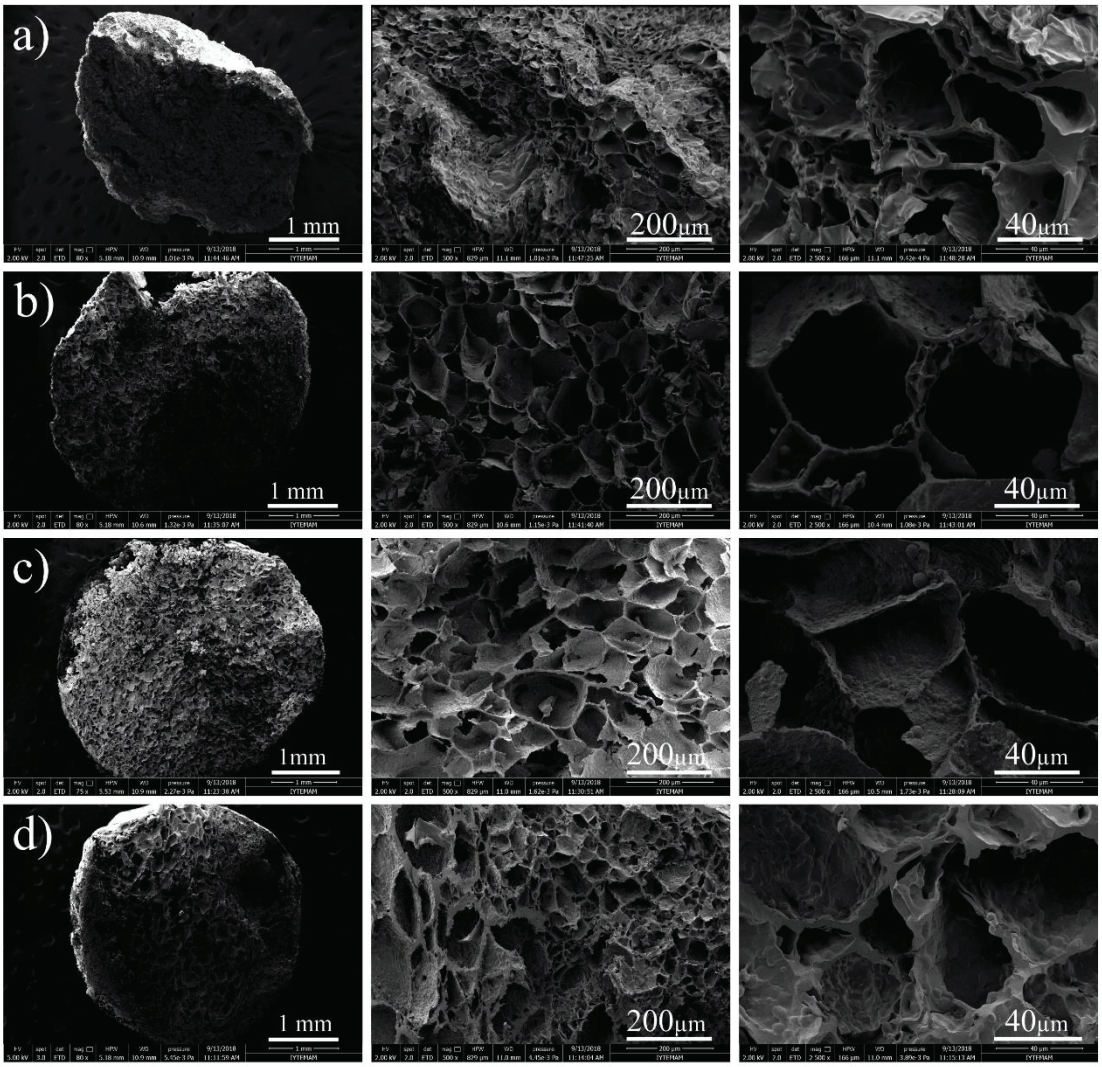

Figure 3.19 SEM images of GelatinK3 hydrogels in different polymer concentrations. a) 5% (w/v), b) 7.5% (w/v), c) 10% (w/v), d) 15% (w/v).

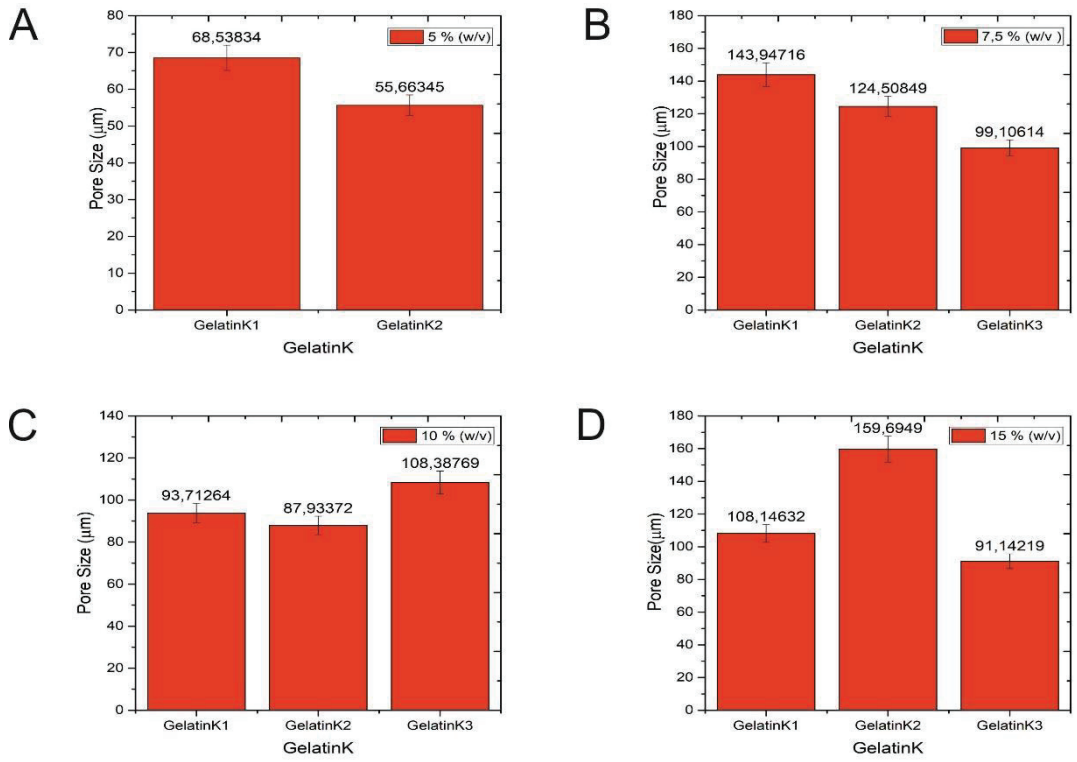

Figure 3.20 Pore sizes (µm) of GelatinK hydrogels with concentration of; a) 5% (w/v), b) 7.5% (w/v), c) 10% (w/v), d) 15% (w/v) GelatinK polymer.

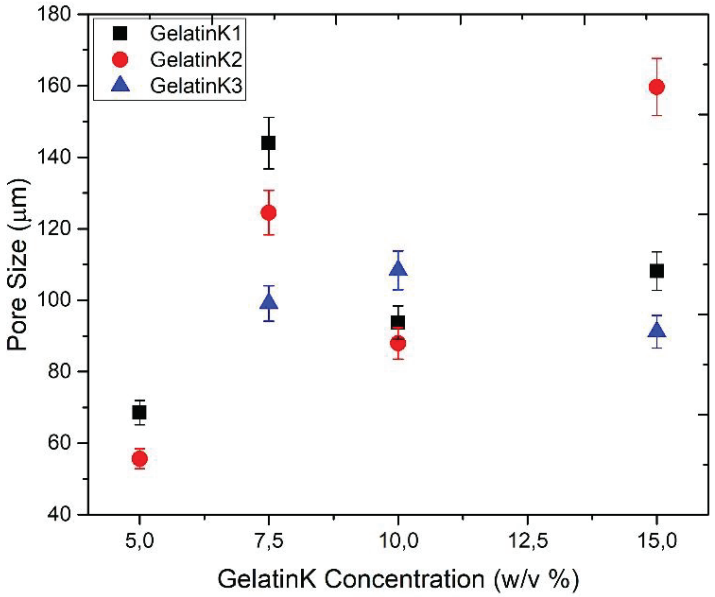

Figure 3.21 Pore sizes (µm) of GelatinK1, GelatinK2 and GelatinK3 hydrogels.

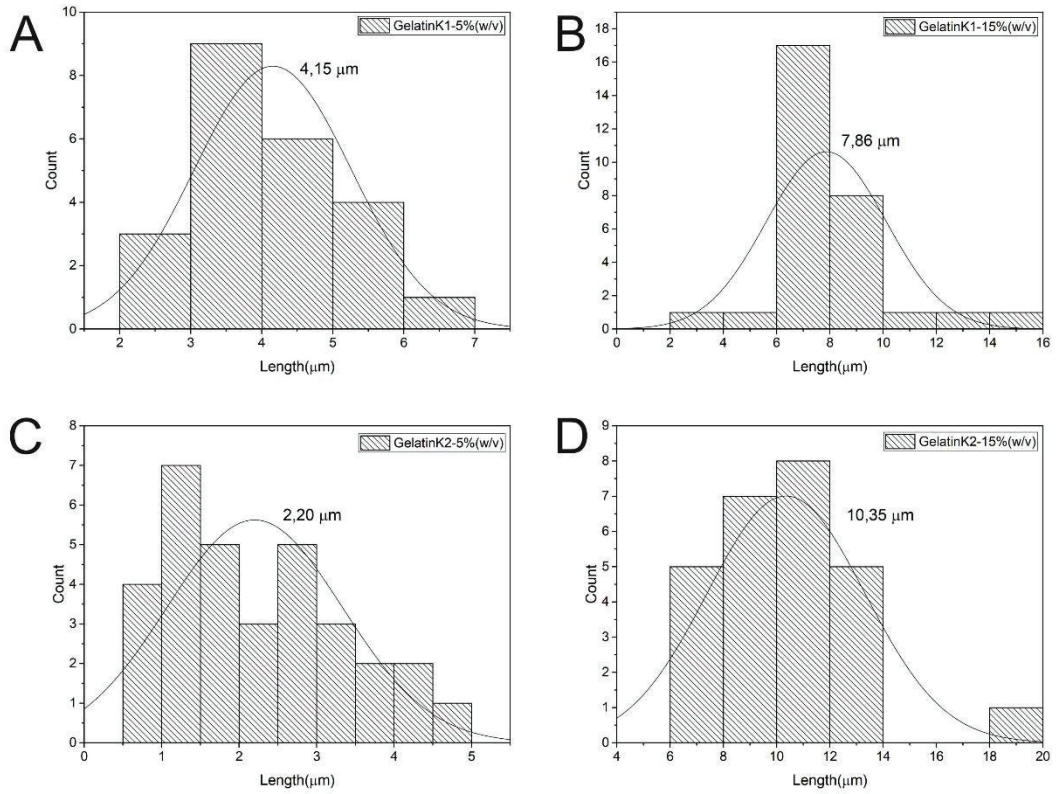

Figure 3.22 Pore wall length of GelatinK hydrogels. a) GelatinK1 5% (w/v), b) GelatinK1 15% (w/v), c) GelatinK2 5% (w/v), d) GelatinK2 15% (w/v).

Amino groups are able to capture H^+ and polymer chains gets far from each other absorbing water into the gap between polymer chains and hydrogel swells in water. For example in 5% (w/v) polymer concentration, GelMA1, GelMA2, GelMA3, GelMA4 and GelMA5 has nearly 1156, 615, 421, 314 and 336% swelling capacity respectively. This decreasing trend are also seen in 7.5%, 10% and 15% polymer concentrations.

Figure 3.24 demonstrates percent swelling ratio (%SR) of all GelMA hydrogel formulations with varying methacrylation and concentrations in a single graph. As clearly seen from the graph, methacrylation decreases the swelling ability of GelMA hydrogel whereas polymer concentration in hydrogel affects swelling ratio positively. When polymer concentration in %1 Irgacure solution is increased during gelation, equilibrium swelling ratio of hydrogel will increase regardless of methacrylation degree of gelatin. In GelMA1, swelling ratio decreases from 1155 to 1041% when polymer concentration increases from 5% to 15% (w/v). In GelMA2, 5% (w/v) gel has nearly 615% and 15% gel has nearly 557% swelling ratio. The same trend can be seen in all five GelMA concentrations except some deviations in swelling ratio.

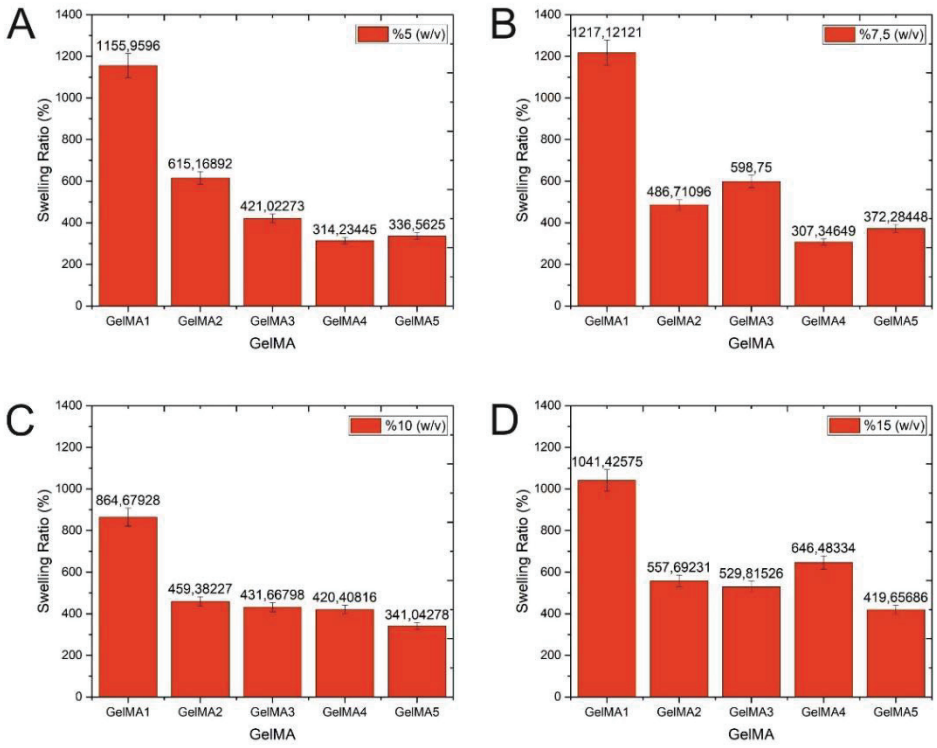

Figure 3.23 Percent swelling ratio of GelMA hydrogels in water produced with different concentrations of GelMA polymer. a) 5% (w/v), b) 7.5% (w/v), c) 10% (w/v), d) 15% (w/v).

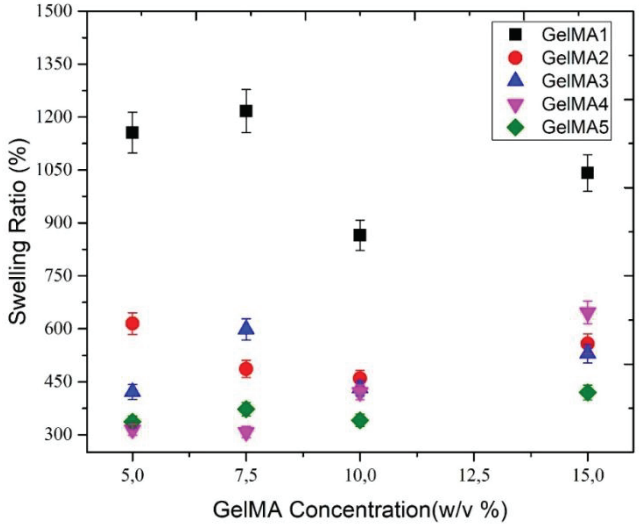

Figure 3.24 Percent swelling ratio of GelMA1, GelMA2, GelMA3, GelMA4 and GelMA5 hydrogels in water produced with different concentrations of GelMA polymer.

Percent swelling ratio of GelatinK hydrogels is shown in Figure 3.25 and Figure 3.26. %SR of hydrogels show a downward pattern from GelatinK3 to GelatinK1. In GelatinK backbone, number of amino groups rise after modification of gelatin with 2-isocyanatoethyl methacrylate (Figure 2.2). Since the swelling of hydrogels occurs via capture of H^+ by amino groups, swelling ability of GelatinK hydrogels with higher modification rises from GelatinK1 to GelatinK3. This trend in %SR is reverse of that of GelMA hydrogels. As an example, GelatinK3 has nearly 1900% while GelatinK2 and GelatinK1 have nearly 1100 and 900% swelling ratio respectively in 5% (w/v) polymer concentration (Figure 3.26). In addition, swelling ability of GelatinK hydrogels declines when polymer concentration increases (Figure 3.26). For instance, GelatinK1 hydrogels has nearly 918%, 676%, 568% and 461% swelling ratios in 5, 7.5, 10 and 15% (w/v) polymer concentrations respectively. GelatinK2 and GelatinK3 hydrogels follow the same decreasing trend in swelling capacity in response to increasing polymer concentration.

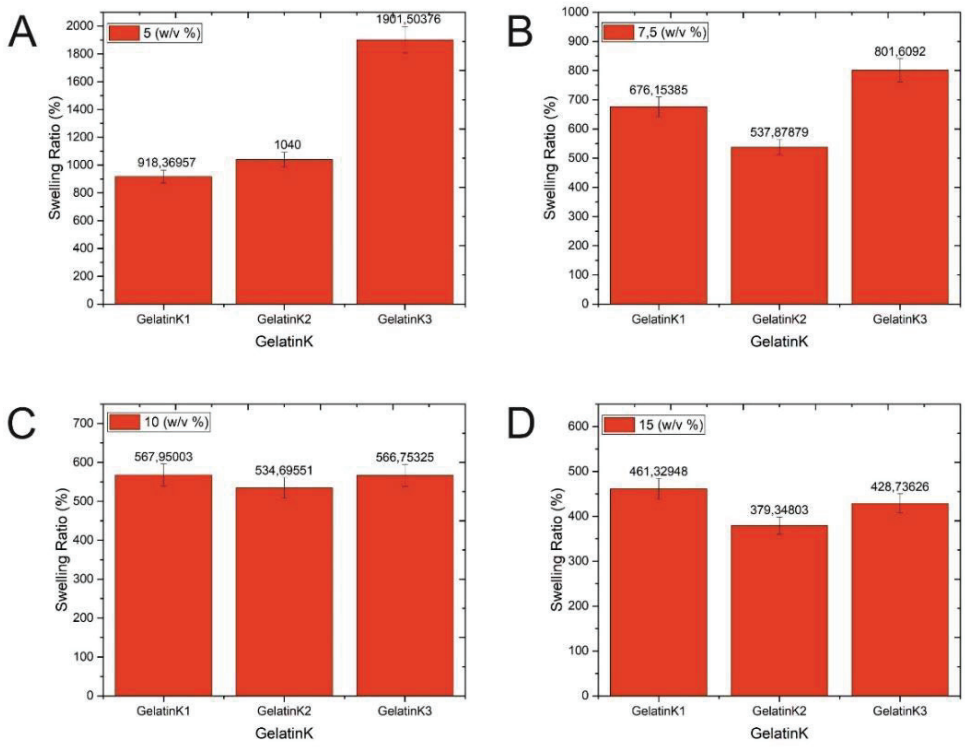

Figure 3.25 Percent swelling ratio of GelatinK hydrogels in water produced with different concentrations of GelatinK polymer. a) 5% (w/v), b) 7.5% (w/v), c) 10% (w/v), d) 15% (w/v).

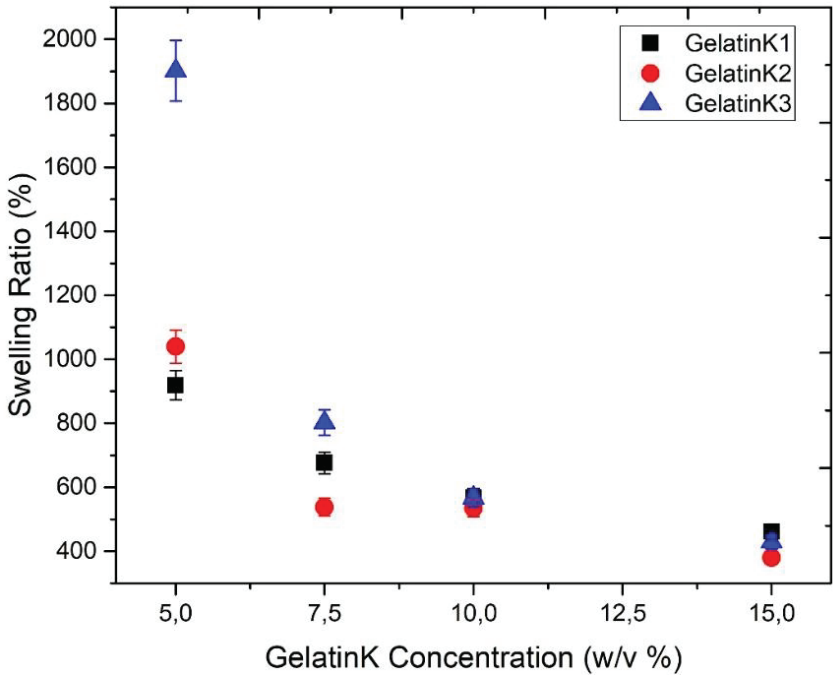

Figure 3.26 Percent swelling ratio of GelatinK1, GelatinK2 and GelatinK3 hydrogels in water produced with different concentrations of GelMA polymer.

For instance, GelatinK1 hydrogels has nearly 918%, 676%, 568% and 461% swelling ratios in 5, 7.5, 10 and 15% (w/v) polymer concentrations respectively. GelatinK2 and GelatinK3 hydrogels follow the same decreasing trend in swelling capacity in response to increasing polymer concentration. The possible reason for this decrease is that increasing density of polymer backbone in hydrogel can hinder capture of proton by amino groups. Due to this hindrance, swelling capacity of hydrogels drops with increasing polymer concentration in the hydrogel.

3.6. Cell Viability Assay

Cell viability experiments were conducted with GelMA hydrogels to see the toxicity of hydrogels for NIH 3T3 mouse fibroblast cells. GelMA hydrogels were freshly synthesized in well plates with 40 µl polymer solution under 5 min UV curing. Cells were seeded on hydrogels in well plates with three replicates and 2D control group. Figure 3.27 demonstrates cell viability results after 24 hours incubation of cells on hydrogel. As seen, cell viability decreases from GelMA1 to GelMA5. For instance, GelMA1, GeMA2, GelMA3, GelMA4 and GelMA5 hydrogels have nearly 37, 30, 24, 19 and 28% cell viabilities respectively.

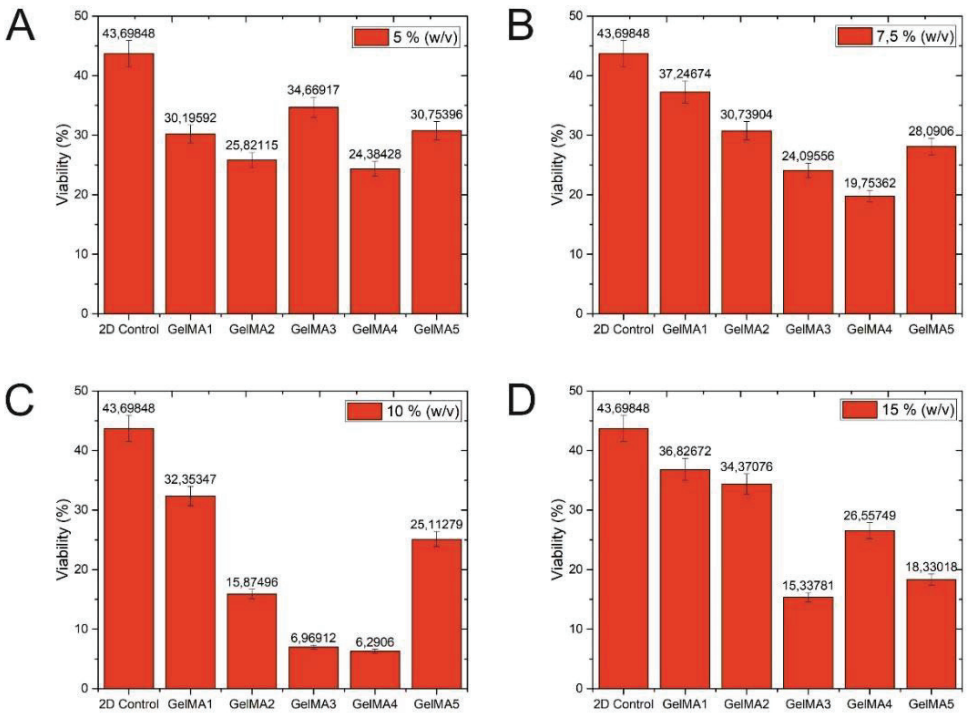

Figure 3.27 Cell viability results of GelMA hydrogels after 24h incubation. a) 5% (w/v), b) 7.5% (w/v), c) 10% (w/v), d) 15% (w/v).

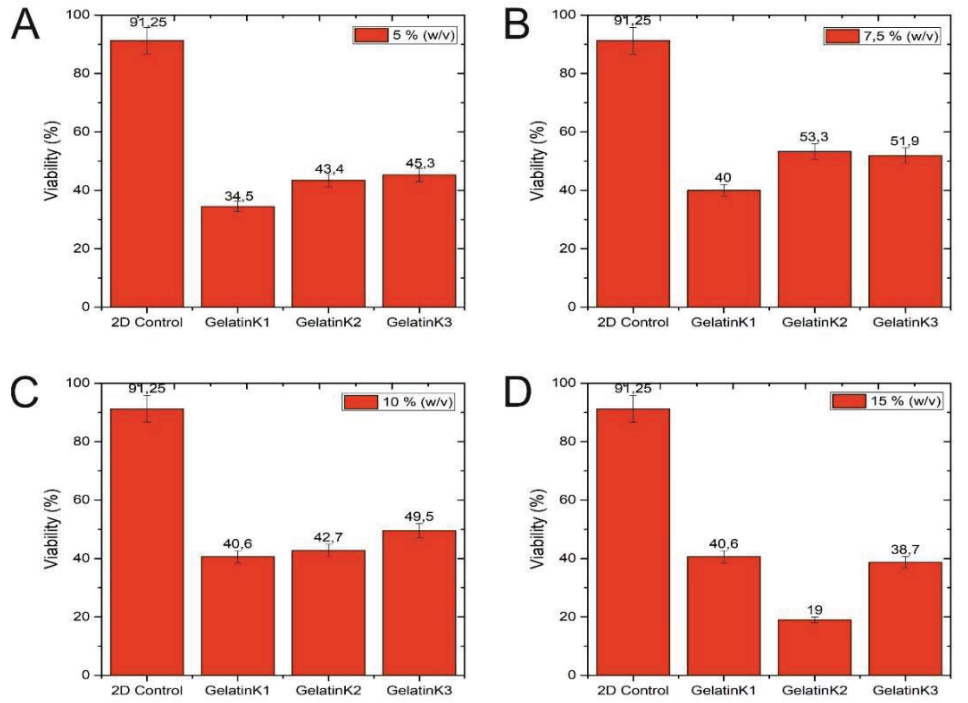

Figure 3.28 Cell viability results of GelatinK hydrogels after 24h incubation. a) 5% (w/v), b) 7.5% (w/v), c) 10% (w/v), d) 15% (w/v).

Also, viability decreases from nearly 37 to 18% in 15% (w/v) gels going from GelMA1 to GelMA5. All hydrogel formulations demonstrate same declining trend in cell viability except some deviations due to experimental errors like homogeneity problem in gel or incubation period. Also, biocompatibility of GelatinK hydrogels were examined with same procedure as in GelMA hydrogels. Figure 3.28 shows cell viability results after 24 hours incubation of cells on GelatinK hydrogels. For example, in 7.5% (w/v) gels, GelatinK1, GelatinK2 and GelatinK3 have 40, 53.3 and 51.9% viabilities respectively. The GelatinK hydrogels are as biocompatible as GelMA hydrogels according to cell viability results.

The relatively low cell viabilities on the hydrogels can be due to the low transport of cell medium and oxygen. The pore size and interconnectivity of pores affect the mass transport during cell culturing. Also, the modification of gelatin with methacrylic anhydride and Karenz can lead toxic effect on NIH 3T3 cells.

CHAPTER 4

CONCLUSION

Hydrogel-based soft-materials provide high biocompatibility and functionality with their chemical, physical/biophysical properties for tissue engineering applications. Hydrogels are produced using synthetic, natural or hybrid materials to construct desired 3D scaffold mimicking specific tissue or organ model. Their responsiveness, porous morphology, mechanical properties and swelling ability make the hydrogels a suitable candidate for a scaffold. Due to their tunable properties and biocompatibility, gelatin based hydrogels were selected as scaffold material. However, gelatin should be modified with proper reagents due to high solubility in aqueous media results mechanically weak hydrogels. In this study, gelatin was modified with two different reagents which are methacrylic anhydride (MA) and 2-isocyanatoethyl methacrylate (Karenz) to see differences between modifications on backbone. Modification degree of gelatin backbone is changed by increasing MA and Karenz ratio in synthesis procedure. FTIR results show that gelatin was successfully modified.

Using GelMA and GelatinK polymers, GelMA and GelatinK hydrogels were synthesized with photopolymerization reactions in aqueous media to prevent toxicity of other organic solvent and reagents. Polymerization time is observed as 5 min for GelMA and 2 min for GelatinK hydrogels and this shows higher reactivity of GelatinK polymer compared to GelMA polymer. Hydrogels were freeze dried for morphology analysis and swelling experiments. SEM analysis proof that all GelMA and GelatinK hydrogels are porous with different pore sizes. Pore size distributions are almost same for GelMA and GelatinK. Furthermore, swelling measurements explain that GelatinK hydrogels have more swelling capacity than GelMA hydrogels. This result is possibly due to that GelatinK backbone has more NH groups on GelMA backbone so proton gets higher in GelatinK hydrogels. Furthermore, cell viability results demonstrate biocompatibilities of both GelMA and GelatinK hydrogels with relatively high viabilities of NIH 3T3 mouse fibroblast cells on scaffold.

As a conclusion, novel gelatin based hydrogels were designed and characterized using FTIR, SEM imaging, swelling experiments and cell culture experiments. It can be said that GelMA and GelatinK hydrogels are possible scaffolds for tissue engineering applications with high porosity, excellent swelling capacity and biocompatibility. Also, tunable properties of these hydrogels allow to fabricating varied hydrogel formulations according to demand on specific tissue an organ models.

REFERENCES

1. Demirdirek, B.; Uhrich, K. E., Novel salicylic acid-based chemically crosslinked pH-sensitive hydrogels as potential drug delivery systems. Int J Pharm 2017, 528 (1-2), 406-415.

2. Sarkar, N.; Sahoo, G.; Das, R.; Prusty, G.; Swain, S. K., Carbon quantum dot tailored calcium alginate hydrogel for pH responsive controlled delivery of vancomycin. Eur J Pharm Sci 2017, 109, 359-371.

3. Quan, S.; Wang, Y.; Zhou, A.; Kumar, P.; Narain, R., Galactose-based Thermosensitive Nanogels for Targeted Drug Delivery of Iodoazomycin Arabinofuranoside (IAZA) for Theranostic Management of Hypoxic Hepatocellular Carcinoma. Biomacromolecules 2015, 16 (7), 1978-86.

4. Ruel-Gariépy, E.; Shive, M.; Bichara, A.; Berrada, M.; Le Garrec, D.; Chenite, A.; Leroux, J.-C., A thermosensitive chitosan-based hydrogel for the local delivery of paclitaxel. European Journal of Pharmaceutics and Biopharmaceutics 2004, 57 (1), 53-63.

5. Koetting, M. C.; Guido, J. F.; Gupta, M.; Zhang, A.; Peppas, N. A., pH-responsive and enzymatically-responsive hydrogel microparticles for the oral delivery of therapeutic proteins: Effects of protein size, crosslinking density, and hydrogel degradation on protein delivery. J Control Release 2016, 221, 18-25.

6. Zou, X.; Zhao, X.; Ye, L., Synthesis of cationic chitosan hydrogel and its controlled glucose-responsive drug release behavior. Chemical Engineering Journal 2015, 273, 92-100.

7. Jackson, N.; Stam, F., Optimization of electrical stimulation parameters for electro-responsive hydrogels for biomedical applications. Journal of Applied Polymer Science 2014, n/a-n/a.

8. Rahimi, N.; Molin, D. G.; Cleij, T. J.; van Zandvoort, M. A.; Post, M. J., Electrosensitive polyacrylic acid/fibrin hydrogel facilitates cell seeding and alignment. Biomacromolecules 2012, 13 (5), 1448-57.

9. Chiang, C. Y.; Chu, C. C., Synthesis of photoresponsive hybrid alginate hydrogel with photo-controlled release behavior. Carbohydr Polym 2015, 119, 18-25.

10. Hang, C.; Zou, Y.; Zhong, Y.; Zhong, Z.; Meng, F., NIR and UV-responsive degradable hyaluronic acid nanogels for CD44-targeted and remotely triggered intracellular doxorubicin delivery. Colloids Surf B Biointerfaces 2017, 158, 547-555.

11. Wang, C.; Zhang, G.; Liu, G.; Hu, J.; Liu, S., Photo- and thermo-responsive multicompartment hydrogels for synergistic delivery of gemcitabine and doxorubicin. J Control Release 2017, 259, 149-159.

12. Wang, L.; Liu, M.; Gao, C.; Ma, L.; Cui, D., A pH-, thermo-, and glucose-, triple-responsive hydrogels: Synthesis and controlled drug delivery. Reactive and Functional Polymers 2010, 70 (3), 159-167.

13. Wei, W.; Li, J.; Qi, X.; Zhong, Y.; Zuo, G.; Pan, X.; Su, T.; Zhang, J.; Dong, W., Synthesis and characterization of a multi-sensitive polysaccharide hydrogel for drug delivery. Carbohydr Polym 2017, 177, 275-283.

14. Zhang, Q.; Colazo, J.; Berg, D.; Mugo, S. M.; Serpe, M. J., Multiresponsive Nanogels for Targeted Anticancer Drug Delivery. Mol Pharm 2017, 14 (8), 2624-2628.

15. Wu, T.; Huang, J.; Jiang, Y.; Hu, Y.; Ye, X.; Liu, D.; Chen, J., Formation of hydrogels based on chitosan/alginate for the delivery of lysozyme and their antibacterial activity. Food Chem 2018, 240, 361-369.

16. Alemdar, N., Fabrication of a novel bone ash-reinforced gelatin/alginate/hyaluronic acid composite film for controlled drug delivery. Carbohydr Polym 2016, 151, 1019-1026.

17. George, S. M.; Moon, H., Digital microfluidic three-dimensional cell culture and chemical screening platform using alginate hydrogels. Biomicrofluidics 2015, 9 (2), 024116.

18. Li, Y.; Feng, C.; Li, J.; Mu, Y.; Liu, Y.; Kong, M.; Cheng, X.; Chen, X., Construction of multilayer alginate hydrogel beads for oral delivery of probiotics cells. Int J Biol Macromol 2017, 105 (1), 924-930.

19. Hou, J.; Hong, Z.; Feng, F.; Chai, Y.; Zhang, Y.; Jiang, Q.; Hu, Y.; Wu, S.; Wu, Y.; Gao, X.; Chen, Q.; Wan, Y.; Bi, J.; Zhang, Z., A novel chemotherapeutic sensitivity-testing system based on collagen gel droplet embedded 3D-culture methods for hepatocellular carcinoma. BMC Cancer 2017, 17 (1), 729.

20. Yang, X.; Lu, Z.; Wu, H.; Li, W.; Zheng, L.; Zhao, J., Collagen-alginate as bioink for three-dimensional (3D) cell printing based cartilage tissue engineering. Mater Sci Eng C Mater Biol Appl 2018, 83, 195-201.

21. Laha, A.; Sharma, C. S.; Majumdar, S., Electrospun gelatin nanofibers as drug carrier: effect of crosslinking on sustained release. Materials Today: Proceedings 2016, 3 (10), 3484-3491.

22. Lien, S.-M.; Li, W.-T.; Huang, T.-J., Genipin-crosslinked gelatin scaffolds for articular cartilage tissue engineering with a novel crosslinking method. Materials Science and Engineering: C 2008, 28 (1), 36-43.

23. Yang, M.; Wu, J.; Bai, H.; Xie, T.; Zhao, Q.; Wong, T.-W., Controlling three-dimensional ice template via two-dimensional surface wetting. AIChE Journal 2016, 62 (12), 4186-4192.

24. Allan, I. U.; Tolhurst, B. A.; Shevchenko, R. V.; Dainiak, M. B.; Illsley, M.; Ivanov, A.; Jungvid, H.; Galaev, I. Y.; James, S. L.; Mikhalovsky, S. V.; James, S. E., An in vitro evaluation of fibrinogen and gelatin containing cryogels as dermal regeneration scaffolds. Biomater Sci 2016, 4 (6), 1007-14.

25. Juan Li, S. Y., Ping Yao, and Ming Jiang, Lysozyme-Dextran Core-Shell Nanogels Prepared via a Green Process. Langmuir 2008, 24 (7), 3486-3492.

26. Liu, J.; Qi, C.; Tao, K.; Zhang, J.; Zhang, J.; Xu, L.; Jiang, X.; Zhang, Y.; Huang, L.; Li, Q.; Xie, H.; Gao, J.; Shuai, X.; Wang, G.; Wang, Z.; Wang, L., Sericin/Dextran Injectable Hydrogel as an Optically Trackable Drug Delivery System for Malignant Melanoma Treatment. ACS Appl Mater Interfaces 2016, 8 (10), 6411-22.

27. Highley, C. B.; Prestwich, G. D.; Burdick, J. A., Recent advances in hyaluronic acid hydrogels for biomedical applications. Current Opinion in Biotechnology 2016, 40, 35-40.

28. Xiao, L.; Tong, Z.; Chen, Y.; Pochan, D. J.; Sabanayagam, C. R.; Jia, X., Hyaluronic acid-based hydrogels containing covalently integrated drug depots: implication for controlling inflammation in mechanically stressed tissues. Biomacromolecules 2013, 14 (11), 3808-19.

29. Ahmed, E. M., Hydrogel: Preparation, characterization, and applications: A review. J Adv Res 2015, 6 (2), 105-21.

30. Goh, K. B.; Li, H.; Lam, K. Y., Development of a multiphysics model to characterize the responsive behavior of urea-sensitive hydrogel as biosensor. Biosens Bioelectron 2017, 91, 673-679.

31. Spizzirri, U. G.; Hampel, S.; Cirillo, G.; Nicoletta, F. P.; Hassan, A.; Vittorio, O.; Picci, N.; Iemma, F., Spherical gelatin/CNTs hybrid microgels as electro-responsive drug delivery systems. Int J Pharm 2013, 448 (1), 115-22.

32. Tan, B. H.; Ravi, P.; Tam, K. C., Synthesis and Characterization of Novel pH-Responsive Polyampholyte Microgels. Macromolecular Rapid Communications 2006, 27 (7), 522-528.

33. Yin, R.; Wang, K.; Du, S.; Chen, L.; Nie, J.; Zhang, W., Design of genipin-crosslinked microgels from concanavalin A and glucosyloxyethyl acrylated chitosan for glucose-responsive insulin delivery. Carbohydr Polym 2014, 103, 369-76.

34. Manchun, S.; Dass, C. R.; Cheewatanakornkool, K.; Sriamornsak, P., Enhanced anti-tumor effect of pH-responsive dextrin nanogels delivering doxorubicin on colorectal cancer. Carbohydr Polym 2015, 126, 222-30.

35. Lim, H.-P.; Ooi, C.-W.; Tey, B.-T.; Chan, E.-S., Controlled delivery of oral insulin aspart using pH-responsive alginate/κ-carrageenan composite hydrogel beads. Reactive and Functional Polymers 2017, 120, 20-29.

36. Lu, Q.; Zhang, S.; Xiong, M.; Lin, F.; Tang, L.; Huang, B.; Chen, Y., One-pot construction of cellulose-gelatin supramolecular hydrogels with high strength and pH-responsive properties. Carbohydrate Polymers 2018, 196, 225-232.

37. Ullah, F.; Othman, M. B.; Javed, F.; Ahmad, Z.; Md Akil, H., Classification, processing and application of hydrogels: A review. Mater Sci Eng C Mater Biol Appl 2015, 57, 414-33.

38. Lue, S. J.; Chen, C.-H.; Shih, C.-M., Tuning of Lower Critical Solution Temperature (LCST) of Poly(N-Isopropylacrylamide-co-Acrylic acid) Hydrogels. Journal of Macromolecular Science, Part B 2011, 50 (3), 563-579.

39. Ulijn, R. V., Enzyme-responsive materials: a new class of smart biomaterials. Journal of Materials Chemistry 2006, 16 (23).

40. Yan Liu, J. L. V., Malcolm B. Huglin, Thermoreversible swelling behaviour of hydrogels based on N-isopropylacrylamide with sodium acrylate and sodium methacrylate. Polymer 1999, 40, 4299-4306.

41. Wu, W.; Zhou, S., Hybrid micro-/nanogels for optical sensing and intracellular imaging. Nano Rev 2010, 1.

42. Xiong, M.-H.; Li, Y.-J.; Bao, Y.; Yang, X.-Z.; Hu, B.; Wang, J., Bacteria-Responsive Multifunctional Nanogel for Targeted Antibiotic Delivery. Advanced Materials 2012, 24 (46), 6175-6180.

43. Chen, J.; Gao, L.-x.; Han, X.; Chen, T.; Luo, J.; Liu, K.; Gao, Z.; Zhang, W., Preparation and electro-response of chitosan-g-poly (acrylic acid) hydrogel elastomers with interpenetrating network. Materials Chemistry and Physics 2016, 169, 105-112.

44. Gao, Y.; Xu, S.; Wu, R.; Wang, J.; Wei, J., Preparation and characteristic of electric stimuli responsive hydrogel composed of polyvinyl alcohol/poly (sodium maleate-co-sodium acrylate). Journal of Applied Polymer Science 2008, 107 (1), 391-395.

45. Jing Shang, Z. S., and Xin Chen, Electrical Behavior of a Natural Polyelectrolyte Hydrogel: Chitosan/Carboxymethylcellulose Hydrogel. Biomacromolecules 2008, 9 (4), 1208-1213.

46. Gao, L. X.; Chen, J. L.; Han, X. W.; Yan, S. X.; Zhang, Y.; Zhang, W. Q.; Gao, Z. W., Electro-response characteristic of starch hydrogel crosslinked with Glutaraldehyde. J Biomater Sci Polym Ed 2015, 26 (9), 545-57.

47. Bahram, M.; Mohseni, N.; Moghtader, M., An Introduction to Hydrogels and Some Recent Applications. In Emerging Concepts in Analysis and Applications of Hydrogels, 2016.

48. Kang, H.; Trondoli, A. C.; Zhu, G.; Chen, Y.; Chang, Y. J.; Liu, H.; Huang, Y. F.; Zhang, X.; Tan, W., Near-infrared light-responsive core-shell nanogels for targeted drug delivery. ACS Nano 2011, 5 (6), 5094-9.

49. Zhang, Y.-W.; Guan, W.-J.; Lu, Y.-M.; Zhao, J.-X., Efficient and "green" fabrication of pH-responsive poly(methacrylic acid) nano-hydrogels in water. RSC Advances 2016, 6 (71), 66571-66578.

50. Koetting, M. C.; Peters, J. T.; Steichen, S. D.; Peppas, N. A., Stimulus-responsive hydrogels: Theory, modern advances, and applications. Mater Sci Eng R Rep 2015, 93, 1-49.

51. Erman, B.; Flory, P. J., Theory of elasticity of polymer networks. II. The effect of geometric constraints on junctions. The Journal of Chemical Physics 1978, 68 (12), 5363-5369.

52. Kang, T.; Li, F.; Baik, S.; Shao, W.; Ling, D.; Hyeon, T., Surface design of magnetic nanoparticles for stimuli-responsive cancer imaging and therapy. Biomaterials 2017, 136, 98-114.

53. Scherer, G. W., Structure and properties of gels. Cement and Concrete Research 1999, 29 (8), 1149-1157.

54. Yadollahi, M.; Gholamali, I.; Namazi, H.; Aghazadeh, M., Synthesis and characterization of antibacterial carboxymethylcellulose/CuO bio-nanocomposite hydrogels. Int J Biol Macromol 2015, 73, 109-14.

55. Coutinho, D. F.; Sant, S. V.; Shin, H.; Oliveira, J. T.; Gomes, M. E.; Neves, N. M.; Khademhosseini, A.; Reis, R. L., Modified Gellan Gum hydrogels with tunable physical and mechanical properties. Biomaterials 2010, 31 (29), 7494-502.

56. Hachet, E.; Van Den Berghe, H.; Bayma, E.; Block, M. R.; Auzely-Velty, R., Design of biomimetic cell-interactive substrates using hyaluronic acid hydrogels with tunable mechanical properties. Biomacromolecules 2012, 13 (6), 1818-27.

57. You, J.; Xie, S.; Cao, J.; Ge, H.; Xu, M.; Zhang, L.; Zhou, J., Quaternized Chitosan/Poly(acrylic acid) Polyelectrolyte Complex Hydrogels with Tough, Self-Recovery, and Tunable Mechanical Properties. Macromolecules 2016, 49 (3), 1049-1059.

58. De France, K. J.; Chan, K. J.; Cranston, E. D.; Hoare, T., Enhanced Mechanical Properties in Cellulose Nanocrystal-Poly(oligoethylene glycol methacrylate) Injectable Nanocomposite Hydrogels through Control of Physical and Chemical Cross-Linking. Biomacromolecules 2016, 17 (2), 649-60.

59. Tang, S.; Glassman, M. J.; Li, S.; Socrate, S.; Olsen, B. D., Oxidatively Responsive Chain Extension to Entangle Engineered Protein Hydrogels. Macromolecules 2014, 47 (2), 791-799.

60. Langer, R.; Vacanti, J. P., Tissue engineering. Science (New York, N.Y.) 1993, 260 (5110), 920-6.

61. Arslan-Yildiz, A.; El Assal, R.; Chen, P.; Guven, S.; Inci, F.; Demirci, U., Towards artificial tissue models: past, present, and future of 3D bioprinting. Biofabrication 2016, 8 (1), 014103.

62. Guan, X.; Avci-Adali, M.; Alarçin, E.; Cheng, H.; Kashaf, S. S.; Li, Y.; Chawla, A.; Jang, H. L.; Khademhosseini, A., Development of hydrogels for regenerative engineering. Biotechnology journal 2017, 12 (5), 10.1002/biot.201600394.

63. Howard, D.; Buttery, L. D.; Shakesheff, K. M.; Roberts, S. J., Tissue engineering: strategies, stem cells and scaffolds. Journal of anatomy 2008, 213 (1), 66-72.

64. Verhulsel, M.; Vignes, M.; Descroix, S.; Malaquin, L.; Vignjevic, D. M.; Viovy, J.-L., A review of microfabrication and hydrogel engineering for micro-organs on chips. Biomaterials 2014, 35 (6), 1816-1832.

65. Hoffman, A. S., Hydrogels for biomedical applications. Advanced Drug Delivery Reviews 2012, 64, 18-23.

66. Sharpe, L. A.; Daily, A. M.; Horava, S. D.; Peppas, N. A., Therapeutic applications of hydrogels in oral drug delivery. Expert Opin Drug Deliv 2014, 11 (6), 901-15.

67. Caldorera-Moore, M.; Maass, K.; Hegab, R.; Fletcher, G.; Peppas, N., Hybrid responsive hydrogel carriers for oral delivery of low molecular weight therapeutic agents. J Drug Deliv Sci Technol 2015, 30 (Pt B), 352-359.

68. Li, Y.; Rodrigues, J.; Tomás, H., Injectable and biodegradable hydrogels: gelation, biodegradation and biomedical applications. Chemical Society Reviews 2012, 41 (6), 2193-2221.

69. Ivanovska, J.; Zehnder, T.; Lennert, P.; Sarker, B.; Boccaccini, A. R.; Hartmann, A.; Schneider-Stock, R.; Detsch, R., Biofabrication of 3D Alginate-Based Hydrogel for Cancer Research: Comparison of Cell Spreading, Viability, and Adhesion Characteristics of Colorectal HCT116 Tumor Cells. Tissue Eng Part C Methods 2016, 22 (7), 708-15.

70. Rhee, S.; Puetzer, J. L.; Mason, B. N.; Reinhart-King, C. A.; Bonassar, L. J., 3D Bioprinting of Spatially Heterogeneous Collagen Constructs for Cartilage Tissue Engineering. ACS Biomaterials Science & Engineering 2016, 2 (10), 1800-1805.

71. Bian, L.; Hou, C.; Tous, E.; Rai, R.; Mauck, R. L.; Burdick, J. A., The influence of hyaluronic acid hydrogel crosslinking density and macromolecular diffusivity on human MSC chondrogenesis and hypertrophy. Biomaterials 2013, 34 (2), 413-421.

72. F., D. C. D.; Andreas, B.; Anne, K.; Sabine, N.; Jörg, J.; Michael, V.; Horst, F., The Stiffness and Structure of Three-Dimensional Printed Hydrogels Direct the Differentiation of Mesenchymal Stromal Cells Toward Adipogenic and Osteogenic Lineages. Tissue Engineering Part A 2015, 21 (3-4), 740-756.

73. Gyles, D. A.; Castro, L. D.; Silva, J. O. C.; Ribeiro-Costa, R. M., A review of the designs and prominent biomedical advances of natural and synthetic hydrogel formulations. European Polymer Journal 2017, 88, 373-392.

74. Bajaj, P.; Schweller, R. M.; Khademhosseini, A.; West, J. L.; Bashir, R., 3D biofabrication strategies for tissue engineering and regenerative medicine. Annual review of biomedical engineering 2014, 16, 247-76.

75. Brougham, C. M.; Levingstone, T. J.; Shen, N.; Cooney, G. M.; Jockenhoevel, S.; Flanagan, T. C.; O'Brien, F. J., Freeze-Drying as a Novel Biofabrication Method for Achieving a Controlled Microarchitecture within Large, Complex Natural Biomaterial Scaffolds. Adv Healthc Mater 2017, 6 (21).

76. Sornkamnerd, S.; Okajima, M. K.; Kaneko, T., Tough and Porous Hydrogels Prepared by Simple Lyophilization of LC Gels. ACS Omega 2017, 2 (8), 5304-5314.

77. Andrea Barbetta, E. B., and Mariella Dentini, Porous Alginate Hydrogels: Synthetic Methods for Tailoring the Porous Texture. Biomacromolecules 2009, 10 (8), 2328–2337.

78. Barbetta, A.; Rizzitelli, G.; Bedini, R.; Pecci, R.; Dentini, M., Porous gelatin hydrogels by gas-in-liquid foam templating. Soft Matter 2010, 6 (8).

79. Lee, S. B.; Kim, Y. H.; Chong, M. S.; Hong, S. H.; Lee, Y. M., Study of gelatin-containing artificial skin V: fabrication of gelatin scaffolds using a salt-leaching method. Biomaterials 2005, 26 (14), 1961-8.

80. De France, K. J.; Xu, F.; Hoare, T., Structured Macroporous Hydrogels: Progress, Challenges, and Opportunities. Adv Healthc Mater 2018, 7 (1).

81. Liao, H.-T.; Shalumon, K. T.; Chang, K.-H.; Sheu, C.; Chen, J.-P., Investigation of synergistic effects of inductive and conductive factors in gelatin-based cryogels for bone tissue engineering. Journal of Materials Chemistry B 2016, 4 (10), 1827-1841.

82. Chang, H. C.; Yang, C.; Feng, F.; Lin, F. H.; Wang, C. H.; Chang, P. C., Bone morphogenetic protein-2 loaded poly(D,L-lactide-co-glycolide) microspheres enhance osteogenic potential of gelatin/hydroxyapatite/beta-tricalcium phosphate cryogel composite for alveolar ridge augmentation. Journal of the Formosan Medical Association = Taiwan yi zhi 2017, 116 (12), 973-981.

83. Raeisdasteh Hokmabad, V.; Davaran, S.; Ramazani, A.; Salehi, R., Design and fabrication of porous biodegradable scaffolds: a strategy for tissue engineering. J Biomater Sci Polym Ed 2017, 28 (16), 1797-1825.

84. Annabi, N.; Nichol, J. W.; Zhong, X.; Ji, C.; Koshy, S.; Khademhosseini, A.; Dehghani, F., Controlling the porosity and microarchitecture of hydrogels for tissue engineering. Tissue engineering. Part B, Reviews 2010, 16 (4), 371-83.

85. Fu, W.; Liu, Z.; Feng, B.; Hu, R.; He, X.; Wang, H.; Yin, M.; Huang, H.; Zhang, H.; Wang, W., Electrospun gelatin/PCL and collagen/PLCL scaffolds for vascular tissue engineering. International Journal of Nanomedicine 2014, 9, 2335-2344.

86. Son, Y. J.; Kim, H. S.; Mao, W.; Park, J. B.; Lee, D.; Lee, H.; Yoo, H. S., Hydro-nanofibrous mesh deep cell penetration: a strategy based on peeling of electrospun coaxial nanofibers. Nanoscale 2018, 10 (13), 6051-6059.

87. Moreira Teixeira, L. S.; Leijten, J. C.; Sobral, J.; Jin, R.; van Apeldoorn, A. A.; Feijen, J.; van Blitterswijk, C.; Dijkstra, P. J.; Karperien, M., High throughput generated micro-aggregates of chondrocytes stimulate cartilage formation in vitro and in vivo. European cells & materials 2012, 23, 387-99.

88. He, J.; Mao, M.; Liu, Y.; Zhu, L.; Li, D., Bottom-up fabrication of 3D cell-laden microfluidic constructs. Materials Letters 2013, 90, 93-96.

89. Cuchiara, M. P.; Gould, D. J.; McHale, M. K.; Dickinson, M. E.; West, J. L., Integration of Self-Assembled Microvascular Networks with Microfabricated PEG-Based Hydrogels. Adv Funct Mater 2012, 22 (21), 4511-4518.

90. Skardal, A.; Murphy, S. V.; Devarasetty, M.; Mead, I.; Kang, H. W.; Seol, Y. J.; Shrike Zhang, Y.; Shin, S. R.; Zhao, L.; Aleman, J.; Hall, A. R.; Shupe, T. D.; Kleensang, A.; Dokmeci, M. R.; Jin Lee, S.; Jackson, J. D.; Yoo, J. J.; Hartung, T.; Khademhosseini, A.; Soker, S.; Bishop, C. E.; Atala, A., Multi-tissue interactions in an integrated three-tissue organ-on-a-chip platform. Sci Rep 2017, 7 (1), 8837.

91. Yanagawa, F.; Sugiura, S.; Kanamori, T., Hydrogel microfabrication technology toward three dimensional tissue engineering. Regenerative Therapy 2016, 3, 45-57.

92. Kang, H. W.; Lee, S. J.; Ko, I. K.; Kengla, C.; Yoo, J. J.; Atala, A., A 3D bioprinting system to produce human-scale tissue constructs with structural integrity. Nat Biotechnol 2016, 34 (3), 312-9.

93. Qi, G.; Eva, T.-C.; Rodrigo, L.; Yu, C.; M., K. R.; Qi, Z.; G., W. G.; M., C. J., Functional 3D Neural Mini-Tissues from Printed Gel-Based Bioink and Human Neural Stem Cells. Advanced Healthcare Materials 2016, 5 (12), 1429-1438.

94. Serra, L.; Domenech, J.; Peppas, N. A., Drug transport mechanisms and release kinetics from molecularly designed poly(acrylic acid-g-ethylene glycol) hydrogels. Biomaterials 2006, 27 (31), 5440-51.

95. Liu, Y.; Chen, X.; Li, S.; Guo, Q.; Xie, J.; Yu, L.; Xu, X.; Ding, C.; Li, J.; Ding, J., Calcitonin-Loaded Thermosensitive Hydrogel for Long-Term Antiosteopenia Therapy. ACS Appl Mater Interfaces 2017, 9 (28), 23428-23440.

96. Yuan, D.; Jacquier, J. C.; O'Riordan, E. D., Entrapment of proteins and peptides in chitosan-polyphosphoric acid hydrogel beads: A new approach to achieve both high entrapment efficiency and controlled in vitro release. Food Chem 2018, 239, 1200-1209.

97. Rehmann, M. S.; Skeens, K. M.; Kharkar, P. M.; Ford, E. M.; Maverakis, E.; Lee, K. H.; Kloxin, A. M., Tuning and Predicting Mesh Size and Protein Release from Step Growth Hydrogels. Biomacromolecules 2017, 18 (10), 3131-3142.

98. Huynh, C. T.; Zheng, Z.; Nguyen, M. K.; McMillan, A.; Yesilbag Tonga, G.; Rotello, V. M.; Alsberg, E., Cytocompatible Catalyst-Free Photodegradable Hydrogels for Light-Mediated RNA Release To Induce hMSC Osteogenesis. ACS Biomaterials Science & Engineering 2017, 3 (9), 2011-2023.

99. Grijalvo, S.; Puras, G.; Zárate, J.; Pons, R.; Pedraz, J. L.; Eritja, R.; Díaz, D. D., Nioplexes encapsulated in supramolecular hybrid biohydrogels as versatile delivery platforms for nucleic acids. RSC Advances 2016, 6 (46), 39688-39699.

100. Wu, W.; Shen, J.; Banerjee, P.; Zhou, S., Core-shell hybrid nanogels for integration of optical temperature-sensing, targeted tumor cell imaging, and combined chemo-photothermal treatment. Biomaterials 2010, 31 (29), 7555-66.

101. Chan, M.; Lux, J.; Nishimura, T.; Akiyoshi, K.; Almutairi, A., Long-Lasting and Efficient Tumor Imaging Using a High Relaxivity Polysaccharide Nanogel Magnetic Resonance Imaging Contrast Agent. Biomacromolecules 2015, 16 (9), 2964-71.

102. Douglas, T. A.; Tamburro, D.; Fredolini, C.; Espina, B. H.; Lepene, B. S.; Ilag, L.; Espina, V.; Petricoin, E. F., 3rd; Liotta, L. A.; Luchini, A., The use of hydrogel microparticles to sequester and concentrate bacterial antigens in a urine test for Lyme disease. Biomaterials 2011, 32 (4), 1157-66.

103. Hah, H. J.; Kim, G.; Lee, Y. E.; Orringer, D. A.; Sagher, O.; Philbert, M. A.; Kopelman, R., Methylene blue-conjugated hydrogel nanoparticles and tumor-cell targeted photodynamic therapy. Macromol Biosci 2011, 11 (1), 90-9.

104. Crulhas, B. P.; Recco, L. C.; Delella, F. K.; Pedrosa, V. A., A Novel Superoxide Anion Biosensor for Monitoring Reactive Species of Oxygen Released by Cancer Cells. Electroanalysis 2017, 29 (5), 1252-1257.

105. Roh, Y. H.; Sim, S. J.; Cho, I. J.; Choi, N.; Bong, K. W., Vertically encoded tetragonal hydrogel microparticles for multiplexed detection of miRNAs associated with Alzheimer's disease. Analyst 2016, 141 (15), 4578-86.

106. Jeong, J.; Kim, H.; Lee, J. B., Enzymatic Polymerization on DNA Modified Gold Nanowire for Label-Free Detection of Pathogen DNA. Int J Mol Sci 2015, 16 (6), 13653-60.

107. Lim, S. L.; Ooi, C.-W.; Tan, W. S.; Chan, E.-S.; Ho, K. L.; Tey, B. T., Biosensing of hepatitis B antigen with poly(acrylic acid) hydrogel immobilized with antigens and antibodies. Sensors and Actuators B: Chemical 2017, 252, 409-417.

108. Kulkarni, A. D.; Joshi, A. A.; Patil, C. L.; Amale, P. D.; Patel, H. M.; Surana, S. J.; Belgamwar, V. S.; Chaudhari, K. S.; Pardeshi, C. V., Xyloglucan: A functional biomacromolecule for drug delivery applications. Int J Biol Macromol 2017, 104 (Pt A), 799-812.

109. Jin, B.; Zhou, X.; Li, X.; Lin, W.; Chen, G.; Qiu, R., Self-Assembled Modified Soy Protein/Dextran Nanogel Induced by Ultrasonication as a Delivery Vehicle for Riboflavin. Molecules (Basel, Switzerland) 2016, 21 (3), 282.

110. Morimoto, N.; Hirano, S.; Takahashi, H.; Loethen, S.; Thompson, D. H.; Akiyoshi, K., Self-assembled pH-sensitive cholesteryl pullulan nanogel as a protein delivery vehicle. Biomacromolecules 2013, 14 (1), 56-63.

111. Nishimura, T.; Yamada, A.; Umezaki, K.; Sawada, S. I.; Mukai, S. A.; Sasaki, Y.; Akiyoshi, K., Self-Assembled Polypeptide Nanogels with Enzymatically Transformable Surface as a Small Interfering RNA Delivery Platform. Biomacromolecules 2017, 18 (12), 3913-3923.

112. C. Gong, T. Q., X. Wei, Y. Qu, Q. Wu, F. Luo and Z. Qian, Thermosensitive Polymeric Hydrogels As Drug Delivery Systems. Current Medicinal Chemistry 2013, 20 (1), 79-94.

113. Hu, Y.; Atukorale, P. U.; Lu, J. J.; Moon, J. J.; Um, S. H.; Cho, E. C.; Wang, Y.; Chen, J.; Irvine, D. J., Cytosolic delivery mediated via electrostatic surface binding of protein, virus, or siRNA cargos to pH-responsive core-shell gel particles. Biomacromolecules 2009, 10 (4), 756-65.

114. Peppas, N. A.; Hilt, J. Z.; Khademhosseini, A.; Langer, R., Hydrogels in Biology and Medicine: From Molecular Principles to Bionanotechnology. Advanced Materials 2006, 18 (11), 1345-1360.

115. Xu, H.; Zhang, J.; Xu, Y.; Wang, H.; Fu, F.; Xu, Q.; Cai, Y., Down's syndrome screening with hydrogel photonic barcodes. Sensors and Actuators B: Chemical 2018, 255, 2690-2696.

116. Wang, H.; Mukherjee, S.; Yi, J.; Banerjee, P.; Chen, Q.; Zhou, S., Biocompatible Chitosan-Carbon Dot Hybrid Nanogels for NIR-Imaging-Guided Synergistic Photothermal-Chemo Therapy. ACS Appl Mater Interfaces 2017, 9 (22), 18639-18649.

117. Jung, I. Y.; Kim, J. S.; Choi, B. R.; Lee, K.; Lee, H., Hydrogel Based Biosensors for In Vitro Diagnostics of Biochemicals, Proteins, and Genes. Adv Healthc Mater 2017, 6 (12).

118. Deligkaris, K.; Tadele, T. S.; Olthuis, W.; van den Berg, A., Hydrogel-based devices for biomedical applications. Sensor Actuat B-Chem 2010, 147 (2), 765-774.

119. Drury; L., J.; Mooney; J., D., Hydrogels for tissue engineering: scaffold design variables and applications. Biomaterials 2003, 24 (24), 4337-4351.

120. Peppas, N. A.; Van Blarcom, D. S., Hydrogel-based biosensors and sensing devices for drug delivery. J Control Release 2016, 240, 142-150.

121. Sorokin, N. V.; Chechetkin, V. R.; Pan'kov, S. V.; Somova, O. G.; Livshits, M. A.; Donnikov, M. Y.; Turygin, A. Y.; Barsky, V. E.; Zasedatelev, A. S., Kinetics of hybridization on surface oligonucleotide microchips: theory, experiment, and comparison with hybridization on gel-based microchips. J Biomol Struct Dyn 2006, 24 (1), 57-66.

122. Srinivas, R. L.; Chapin, S. C.; Doyle, P. S., Aptamer-functionalized microgel particles for protein detection. Anal Chem 2011, 83 (23), 9138-45.

123. Gómez-Guillén, M. C.; Giménez, B.; López-Caballero, M. E.; Montero, M. P., Functional and bioactive properties of collagen and gelatin from alternative sources: A review. Food Hydrocolloids 2011, 25 (8), 1813-1827.

124. Theocharis, A. D.; Skandalis, S. S.; Gialeli, C.; Karamanos, N. K., Extracellular matrix structure. Adv Drug Deliv Rev 2016, 97, 4-27.

125. Cicha, I.; Detsch, R.; Singh, R.; Reakasame, S.; Alexiou, C.; Boccaccini, A. R., Biofabrication of vessel grafts based on natural hydrogels. Current Opinion in Biomedical Engineering 2017, 2, 83-89.

126. Nichol, J. W.; Koshy, S. T.; Bae, H.; Hwang, C. M.; Yamanlar, S.; Khademhosseini, A., Cell-laden microengineered gelatin methacrylate hydrogels. Biomaterials 2010, 31 (21), 5536-44.

127. Loessner, D.; Meinert, C.; Kaemmerer, E.; Martine, L. C.; Yue, K.; Levett, P. A.; Klein, T. J.; Melchels, F. P. W.; Khademhosseini, A.; Hutmacher, D. W., Functionalization, preparation and use of cell-laden gelatin methacryloyl–based hydrogels as modular tissue culture platforms. Nature Protocols 2016, 11, 727.

128. Lai, T. C.; Yu, J.; Tsai, W. B., Gelatin methacrylate/carboxybetaine methacrylate hydrogels with tunable crosslinking for controlled drug release. Journal of Materials Chemistry B 2016, 4 (13), 2304-2313.

129. Saraiva, S. M.; Miguel, S. P.; Ribeiro, M. P.; Coutinho, P.; Correia, I. J., Synthesis and characterization of a photocrosslinkable chitosan–gelatin hydrogel aimed for tissue regeneration. RSC Advances 2015, 5 (78), 63478-63488.

130. Cheng, H.; Chabok, R.; Guan, X.; Chawla, A.; Li, Y.; Khademhosseini, A.; Jang, H. L., Synergistic interplay between the two major bone minerals, hydroxyapatite and whitlockite nanoparticles, for osteogenic differentiation of mesenchymal stem cells. Acta Biomaterialia 2018, 69, 342-351.

131. Hosseini, V.; Ahadian, S.; Ostrovidov, S.; Camci-Unal, G.; Chen, S.; Kaji, H.; Ramalingam, M.; Khademhosseini, A., Engineered Contractile Skeletal Muscle Tissue on a Microgrooved Methacrylated Gelatin Substrate. Tissue Engineering Part A 2012, 18 (23-24), 2453-2465.

132. Levato, R.; Webb, W. R.; Otto, I. A.; Mensinga, A.; Zhang, Y.; van Rijen, M.; van Weeren, R.; Khan, I. M.; Malda, J., The bio in the ink: cartilage regeneration with bioprintable hydrogels and articular cartilage-derived progenitor cells. Acta Biomater 2017, 61, 41-53.

133. Kaemmerer, E.; Melchels, F. P.; Holzapfel, B. M.; Meckel, T.; Hutmacher, D. W.; Loessner, D., Gelatine methacrylamide-based hydrogels: an alternative three-dimensional cancer cell culture system. Acta Biomater 2014, 10 (6), 2551-62.

134. Zhao, X.; Lang, Q.; Yildirimer, L.; Lin, Z. Y.; Cui, W.; Annabi, N.; Ng, K. W.; Dokmeci, M. R.; Ghaemmaghami, A. M.; Khademhosseini, A., Photocrosslinkable Gelatin Hydrogel for Epidermal Tissue Engineering. Adv Healthc Mater 2016, 5 (1), 108-18.

135. Klotz, B. J.; Gawlitta, D.; Rosenberg, A.; Malda, J.; Melchels, F. P. W., Gelatin-Methacryloyl Hydrogels: Towards Biofabrication-Based Tissue Repair. Trends Biotechnol 2016, 34 (5), 394-407.

136. Poldervaart, M. T.; Gremmels, H.; van Deventer, K.; Fledderus, J. O.; Öner, F. C.; Verhaar, M. C.; Dhert, W. J. A.; Alblas, J., Prolonged presence of VEGF promotes vascularization in 3D bioprinted scaffolds with defined architecture. Journal of Controlled Release 2014, 184, 58-66.

137. Hassanzadeh, P.; Kazemzadeh-Narbat, M.; Rosenzweig, R.; Zhang, X.; Khademhosseini, A.; Annabi, N.; Rolandi, M., Ultrastrong and flexible hybrid hydrogels based on solution self-assembly of chitin nanofibers in gelatin methacryloyl (GelMA). Journal of Materials Chemistry B 2016, 4 (15), 2539-2543.

138. Kadri, R.; Ben Messaoud, G.; Tamayol, A.; Aliakbarian, B.; Zhang, H. Y.; Hasan, M.; Sánchez-González, L.; Arab-Tehrany, E., Preparation and characterization of nanofunctionalized alginate/methacrylated gelatin hybrid hydrogels. RSC Advances 2016, 6 (33), 27879-27884.

139. Wang, H.; Zhou, L.; Liao, J.; Tan, Y.; Ouyang, K.; Ning, C.; Ni, G.; Tan, G., Cell-laden photocrosslinked GelMA-DexMA copolymer hydrogels with tunable mechanical properties for tissue engineering. Journal of materials science. Materials in medicine 2014, 25 (9), 2173-83.

140. Eslami, M.; Vrana, N. E.; Zorlutuna, P.; Sant, S.; Jung, S.; Masoumi, N.; Khavari-Nejad, R. A.; Javadi, G.; Khademhosseini, A., Fiber-reinforced hydrogel scaffolds for heart valve tissue engineering. Journal of biomaterials applications 2014, 29 (3), 399-410.

141. Sun, G.; Chu, C.-C., Synthesis, characterization of biodegradable dextran–allyl isocyanate–ethylamine/polyethylene glycol–diacrylate hydrogels and their in vitro release of albumin. Carbohydrate Polymers 2006, 65 (3), 273-287.

142. Bandekar, J., Amide modes and protein conformation. Biochimica et Biophysica Acta (BBA) - Protein Structure and Molecular Enzymology 1992, 1120 (2), 123-143.

143. Mad-Ali, S.; Benjakul, S.; Prodpran, T.; Maqsood, S., Characteristics and Gel Properties of Gelatin from Goat Skin as Influenced by Alkaline-pretreatment Conditions. Asian-Australasian journal of animal sciences 2016, 29 (6), 845-54.